REPORT DOCUMENTATION PAGE

Form Approved OMB NO. 0704-0188

1. REPORT DATE (DD-MM-YYYY)	2. REPORT TYPE	3. DATES COVERED (From - To)
22-09-2015	Final Report	1-Sep-2011 - 31-Aug-2015

4. TITLE AND SUBTITLE
Final Report: Development of a Method to Downscale Soil Moisture Estimates based on Topography and Other Site Characteristics

5a. CONTRACT NUMBER
W911NF-11-1-0438

5b. GRANT NUMBER

5c. PROGRAM ELEMENT NUMBER
611102

5d. PROJECT NUMBER

5e. TASK NUMBER

5f. WORK UNIT NUMBER

6. AUTHORS
Garret S. Cowley, Dylan C. Hoehn, Jeffrey D. Niemann, Fredrick A. Busch, Michael L. Coleman, Kevin L. Werbylo, Devin C. Traff, Kayla J. Ranney

7. PERFORMING ORGANIZATION NAMES AND ADDRESSES
Colorado State University - Ft. Collins
Sponsored Programs
2002 Campus Delivery
Fort Collins, CO 80523 -2002

8. PERFORMING ORGANIZATION REPORT NUMBER

9. SPONSORING/MONITORING AGENCY NAME(S) AND ADDRESS (ES)
U.S. Army Research Office
P.O. Box 12211
Research Triangle Park, NC 27709-2211

10. SPONSOR/MONITOR'S ACRONYM(S)
ARO

11. SPONSOR/MONITOR'S REPORT NUMBER(S)
58538-EV.10

12. DISTRIBUTION AVAILIBILITY STATEMENT
Approved for Public Release; Distribution Unlimited

13. SUPPLEMENTARY NOTES
The views, opinions and/or findings contained in this report are those of the author(s) and should not contrued as an official Department of the Army position, policy or decision, unless so designated by other documentation.

14. ABSTRACT
Spatial patterns and dynamics of soil moisture are key factors in the hydrologic behavior of watersheds, and they affect many Army activities including movement of troops in combat and sustainable management of training lands. Yet soil moisture cannot be measured directly at the spatial resolutions and extents that are required for these applications (e.g., 10-100 m grid cells). However, soil moisture is known to depend on topographic attributes and elevation data are widely available at these resolutions. The dependence of soil moisture on topography is complex because it can vary between different regions and between different times in the same region. The

15. SUBJECT TERMS
soil moisture, downscaling, topography, vegetation, soil characteristics, fine resolution

16. SECURITY CLASSIFICATION OF:			17. LIMITATION OF ABSTRACT	15. NUMBER OF PAGES	19a. NAME OF RESPONSIBLE PERSON
a. REPORT	b. ABSTRACT	c. THIS PAGE			Jeffrey Niemann
UU	UU	UU	UU		19b. TELEPHONE NUMBER
					970-491-3517

Report Title

Final Report: Development of a Method to Downscale Soil Moisture Estimates based on Topography and Other Site Characteristics

ABSTRACT

Spatial patterns and dynamics of soil moisture are key factors in the hydrologic behavior of watersheds, and they affect many Army activities including movement of troops in combat and sustainable management of training lands. Yet soil moisture cannot be measured directly at the spatial resolutions and extents that are required for these applications (e.g., 10-100 m grid cells). However, soil moisture is known to depend on topographic attributes and elevation data are widely available at these resolutions. The dependence of soil moisture on topography is complex because it can vary between different regions and between different times in the same region. The objective of this project was to develop and test a downscaling method that estimates high resolution soil moisture patterns based on their dependence on topography and other site characteristics such as soil and vegetation properties if available. This downscaling method overcomes the complex dependence with a simple model that describes the varying influences of the hydrologic processes that determine soil moisture patterns. The method was generalized to be more physically-realistic and broadly-applicable and to better account for the role of vegetation. In addition, it was tested by analyzing underlying assumptions and by comparing against observed soil moisture patterns.

Enter List of papers submitted or published that acknowledge ARO support from the start of the project to the date of this printing. List the papers, including journal references, in the following categories:

(a) Papers published in peer-reviewed journals (N/A for none)

Received		Paper
07/10/2014	6	Kevin L. Werbylo, Jeffrey D. Niemann. Evaluation of sampling techniques to characterize topographically-dependent variability for soil moisture downscaling, Journal of Hydrology, (08 2014): 0. doi: 10.1016/j.jhydrol.2014.01.030
08/23/2013	3	Michael L. Coleman, Jeffrey D. Niemann. Controls on topographic dependence and temporal instability in catchment-scale soil moisture patterns, Water Resources Research, (03 2013): 0. doi: 10.1002/wrcr.20159
08/26/2015	7	Devin C. Traff, Jeffrey D. Niemann, Stephen A. Middlekauff, Brandon M. Lehman. Effects of woody vegetation on shallow soil moisture at a semiarid montane catchment, Ecohydrology, (07 2015): 0. doi: 10.1002/eco.1542
08/26/2015	8	Jeffrey D. Niemann, Brandon M. Lehman, Timothy R. Green, Andrew S. Jones, Kayla J. Ranney. A method to downscale soil moisture to fine resolutions using topographic, vegetation, and soil data, Advances in Water Resources, (02 2015): 0. doi: 10.1016/j.advwatres.2014.12.003

TOTAL: **4**

Number of Papers published in peer-reviewed journals:

(b) Papers published in non-peer-reviewed journals (N/A for none)

Received	Paper

TOTAL:

Number of Papers published in non peer-reviewed journals:

(c) Presentations

Traff, D.C., and J.D. Niemann, April 2013, "Effects of Woody Vegetation on Shallow Soil Moisture at a Semiarid Montane Catchment," American Water Resources Association – Colorado Section, Golden, Colorado.

Traff, D.C., and J.D. Niemann, March 2013, "Effects of Vegetation on Shallow Soil Moisture at a Semiarid Montane Catchment," American Geophysical Union Hydrology Days, Fort Collins, Colorado.

Werbylo, K.L., and J.D. Niemann, March 2013, "Evaluation of Sampling Techniques for Observing Topographically-Dependent Variability in Catchment-Scale Soil Moisture Patterns," American Geophysical Union Hydrology Days, Fort Collins, Colorado.

Werbylo, K.L., and J.D. Niemann, December 2012, "An Efficient Sampling Technique for Observing Topographically-Dependent Spatial Variability in Catchment Scale Soil Moisture Patterns," American Geophysical Union Fall Meeting, San Francisco.

Niemann, J.D., K.J. Ranney, A.S. Jones, T.R. Green, T. Giles, and M. Woodbury, February 2014, "A Framework for Downscaling Intermediate-Resolution Soil Moisture to Fine Resolutions using Topographic, Vegetation, and Soil Information," American Meteorological Society 28th Conference on Hydrology, Atlanta, Georgia.

Ranney, K.J, J.D. Niemann, T.R. Green, and A.S. Jones, March 2014, "Evaluation of a Method to Downscale Intermediate-Resolution Soil Moisture to a Fine Resolution using Topographic, Vegetation, and Soil Data," American Geophysical Union Hydrology Days, Fort Collins, Colorado.

Niemann, J.D., October 2014, "A Framework for Downscaling Intermediate-Resolution Soil Moisture to Fine Resolutions," External Advisory Board Meeting, Department of Civil and Environmental Engineering, Colorado State University, Fort Collins, Colorado.

Niemann, J.D., and M.L. Coleman, November 2014, "On the Origins of Different Types of Topographic Dependence and Temporal Instability in Catchment-Scale Soil Moisture Patterns," International Annual Meeting of the American Society of Agronomy, Crop Science Society of America, and Soil Science Society of America, Long Beach, California.

Number of Presentations: 8.00

Non Peer-Reviewed Conference Proceeding publications (other than abstracts):

Received Paper

TOTAL:

Number of Non Peer-Reviewed Conference Proceeding publications (other than abstracts):

Peer-Reviewed Conference Proceeding publications (other than abstracts):

Received Paper

TOTAL:

Number of Peer-Reviewed Conference Proceeding publications (other than abstracts):

(d) Manuscripts

Received Paper

TOTAL:

Number of Manuscripts:

Books

Received Book

TOTAL:

Received Book Chapter

TOTAL:

Patents Submitted

Patents Awarded

Awards

Graduate Students

NAME	PERCENT_SUPPORTED	Discipline
Kevin Werbylo	0.17	
Devin Traff	0.17	
Kayla Ranney	0.10	
Garret Cowley	0.05	
Michael Coleman	0.08	
FTE Equivalent:	**0.57**	
Total Number:	**5**	

Names of Post Doctorates

NAME	PERCENT_SUPPORTED
FTE Equivalent:	
Total Number:	

Names of Faculty Supported

NAME	PERCENT_SUPPORTED	National Academy Member
Jeffrey D. Niemann	0.08	
FTE Equivalent:	**0.08**	
Total Number:	**1**	

Names of Under Graduate students supported

NAME	PERCENT_SUPPORTED
FTE Equivalent:	
Total Number:	

Student Metrics

This section only applies to graduating undergraduates supported by this agreement in this reporting period

The number of undergraduates funded by this agreement who graduated during this period: 0.00

The number of undergraduates funded by this agreement who graduated during this period with a degree in science, mathematics, engineering, or technology fields:...... 0.00

The number of undergraduates funded by your agreement who graduated during this period and will continue to pursue a graduate or Ph.D. degree in science, mathematics, engineering, or technology fields:...... 0.00

Number of graduating undergraduates who achieved a 3.5 GPA to 4.0 (4.0 max scale):...... 0.00

Number of graduating undergraduates funded by a DoD funded Center of Excellence grant for Education, Research and Engineering:...... 0.00

The number of undergraduates funded by your agreement who graduated during this period and intend to work for the Department of Defense 0.00

The number of undergraduates funded by your agreement who graduated during this period and will receive scholarships or fellowships for further studies in science, mathematics, engineering or technology fields: 0.00

Names of Personnel receiving masters degrees

NAME	
Kevin Werbylo	
Devin Traff	
Kayla Ranney	
Total Number:	**3**

Names of personnel receiving PHDs

NAME	
Michael Coleman	
Total Number:	**1**

Names of other research staff

NAME	PERCENT_SUPPORTED
FTE Equivalent:	
Total Number:	

Sub Contractors (DD882)

Inventions (DD882)

Scientific Progress

See attachment

Technology Transfer

During the project, the downscaling methods were discussed and demonstrated with the Geotechnical and Structures Laboratory (George Mason and others) and the Cold Regions Research and Engineering Laboratory (John Eylander and others). They were also presented to the base managers at Fort Carson (Jeff Linn and others).

Furthermore, the research conducted under this project forms the foundation of an SBIR project that has recently begun to produce commercial software that performs the downscaling algorithm. That SBIR is led by Technology Services Corporation.

Final Report: Development of a Method to Downscale Soil Moisture Estimates based on Topography and Other Site Characteristics

(W911NF-11-1-0438)

Garret S. Cowley[1]
Dylan C. Hoehn[1]
Jeffrey D. Niemann[2]
Fredrick A. Busch
Michael L. Coleman
Kevin L. Werbylo
Devin C. Traff
Kayla J. Ranney

[1]Department of Civil and Environmental Engineering, Colorado State University, Fort Collins, CO 80523, USA

[2]Corresponding author: Department of Civil and Environmental Engineering, Colorado State University, Campus Delivery 1372, Fort Collins, CO 80523, USA, Phone: 970-491-3517, Fax: 970-491-7727, Email: jniemann@engr.colostate.edu

<u>Contents</u>

1. Introduction

It has been shown that soil moisture has significant influence on numerous hydrologic processes including erosion (Fitzjohn et al., 1998), crop yield (Green and Erskine, 2004), the production of surface runoff (Western, 2001), and the partitioning of radiation into sensible and latent heat (Entekhabi et al., 1996). Fine-resolution patterns of soil moisture are essential to applications of water management, agricultural production, and a wide range of Army related activities. Soil moisture affects troop and vehicle mobility in combat, the accuracy of target acquisition systems, and the detection of underground explosives. However, most available methods have not been able to predict soil moisture at the resolutions necessary (10 - 30 m) for many of these applications. For example, the Advanced Microwave Scanning Radiometer (ASMR-E), Soil Moisture and Ocean Salinity (SMOS), WindSat, and Soil Moisture Active Passive (SMAP) satellites can predict soil moisture at 10 km to 60 km resolutions (Kerr et al., 2001; Njoku et al., 2003; Entekhabi et al., 2010; Li et al., 2010). Optical and thermal remote sensing data from MODerate resolution Imaging Spectroradiometer (MODIS) can be used to downscale these estimates to an intermediate resolution (1 km), and remote sensing can obtain soil moisture at a 500 m resolution using algorithms such as the Surface Energy Balance Algorithm for Land (SEBAL) (Merlin et al., 2013; Fang and Lakshmi, 2014; Bastiaanssen et al., 1998; Scott et al., 2003). Additionally, intermediate-resolution (700 m) soil moisture can be obtained from the ground-based Cosmic-ray Soil Moisture Observing System (COSMOS) (Zreda et al., 2008).

To estimate fine-scale variations of soil moisture (resolutions on the order of 10 - 30 m), supplemental high-resolution data are needed that are strongly associated with these variations. Topographic data are widely available at fine resolutions, and it has been shown that topographic attributes influence soil moisture patterns at the catchment scale (Famiglietti et al., 1998;

Western et al., 1999; Erskine et al., 2007; Korres et al., 2010). Wilson et al. (2005) used fine-resolution topographic and in situ soil moisture data in collaboration with a single spatial average soil moisture value on multiple dates to estimate soil moisture patterns at the catchment scale. Similarly, Perry and Niemann (2007) developed a method based on empirical orthogonal function (EOF) analysis to estimate soil moisture patterns based on the average soil moisture for a catchment. In addition, a method was developed by Temimi et al. (2010) to produce high-resolution soil moisture maps using coarse resolution passive microwave sensors, high-resolution terrain-based topographical wetness indices, and vegetation leaf area index maps.

The applicability and the significance of estimating soil moisture at fine resolutions has been clearly defined and explored by numerous researchers and experts, but the methods that have been made available still do not provide dynamic, widely-applicable soil moisture estimates at fine resolutions. Therefore, a method is needed to downscale coarse resolution estimates of soil moisture to resolutions that are appropriate for hydrologic and Army applications. The overarching goal of this project was to develop such a method by addressing the issues of data acquisition, parameter calibration, and soil moisture dependence on multiple variables including topography, soil type, vegetation, and climate. This document only summarizes the main accomplishments of the project. All results have been published in peer-reviewed journal articles, so readers are encouraged to find more information in the references provided throughout this report.

2. Research Objectives

2.1 The EOF Method

The first objective of the project was to determine whether an existing method for soil moisture downscaling could be applied to regions aside from those where it was developed using past high resolution soil moisture observations (i.e. is the method transferrable?). Thus, Busch et al. (2012) extended the research done by Perry and Niemann (2007; 2008), which described a downscaling method that used high-resolution soil moisture data collected from the field to determine empirical orthogonal functions (EOFs). The objective was to develop an EOF-based method to downscale soil moisture using high-resolution topographic data but without requiring high-resolution soil moisture data that was previously collected from the application region.

2.2 Nonlinear Relationships

The second project goal was to evaluate whether nonlinear estimation methods would produce improved performance over previously-used linear estimation methods. There is reason to believe that the relationships between soil moisture and topographic attributes are nonlinear because the topographic attributes in question are generally associated with physical processes that relate nonlinearly to soil moisture (Rodriguez-Iturbe, 2000). The objective of the research done by Coleman and Niemann (2012) was to determine if nonlinear estimation techniques would improve the ability to estimate soil moisture patterns when compared to using multiple linear regression (MLR).

2.3 The EMT Model

The third goal of the project was to devise a new method that overcomes the limitations of the existing empirical downscaling method. After characterizing the capabilities and limitations of the existing empirical downscaling method, a physically-based model was developed to describe the physical processes and dependences of soil moisture in a catchment. The development of this new approach, the Equilibrium Moisture from Topography (EMT) model, was used to investigate the local soil, vegetation, and climatic characteristics that might influence the type of topographic dependence that soil moisture patterns possess at the catchment scale. The model was also used to determine factors that might affect the temporal stability of soil moisture patterns.

2.4 Sampling Techniques

The fourth goal of the project was to examine the data requirements of the newly-developed EMT model. The EOF method relies on large high resolution datasets for its calibration, which might now be available in many cases. The objective of the research done by Werbylo and Niemann (2014) was to evaluate the effectiveness of two strategic sampling techniques at identifying the relationships between topographic attributes and soil moisture at the catchment-scale in order to confine the amount of field data required for the downscaling methods.

2.5 Effects of Vegetation

The fifth goal of the project was to understand how vegetation characteristics might affect soil moisture downscaling. The preceding work developed a better understanding of the relationships between soil moisture and topography, but the effects of vegetation on shallow soil moisture was also investigated. The results from the EOF method and the EMT model both indicated that the soil moisture patterns at the Cache la Poudre catchment were not downscaled as well as the soil moisture patterns at the other application catchments. It was then hypothesized that perhaps topographical attributes alone contributed less to the overall soil moisture dependence at Cache la Poudre. Thus, a study was conducted by Traff et al. (2014) to determine how the presence of shrubs and/or trees affected the shallow soil moisture of the semiarid montane Cache la Poudre catchment at fine resolutions. Why the vegetation caused the observed effects on the soil moisture was also explored.

2.6 The EMT+VS Model

The sixth objective of the project was to incorporate the understanding of vegetation's role into the new downscaling method. Although the EMT model includes vegetation and soil parameters, the model treats them as catchment-wide constants and thus does not consider fine-resolution variations of the properties. The research done by Traff et al. (2014) concluded that soil moisture can be affected by fine-resolution variations of vegetation characteristics, and soil texture variations might have notable effects as well. The objective of the research done by Ranney et al. (2014) was to generalize the EMT model to accept fine-resolution vegetation and soil information so as to improve the model's ability to downscale soil moisture patterns at the catchment-scale. The generalization of the model was called the Equilibrium Moisture from Topography, Vegetation, and Soil (EMT+VS) model.

3. Methods

3.1 The EOF Method

To develop the EOF-based downscaling method, an available dataset for soil moisture on multiple dates and a digital elevation model (DEM) for four specific catchments (Tarrawarra, Tarrawarra 2, Cache la Poudre, and Satellite Station) are used. EOF decomposition is performed on each dataset to identify the patterns of covariation (the EOFs) and their significance on each date (the expansion coefficients or ECs). Using the space-time soil moisture datasets, spatial anomalies are computed by subtracting the spatial average soil moisture from the individual soil moisture values on each date. The anomalies are used to compute a spatial covariance matrix, and an eigenanalysis is performed to create a matrix containing the eigenvectors and a matrix containing the eigenvalues. The eigenvectors are the ECs, which have values associated with each date in the original dataset. The EOFs are new spatial patterns that result from the product of the eigenvectors (the ECs) and the spatial anomalies. Thus, there is an EOF associated with each EC. The number of EOF/EC pairs that are produced is equal to the number of dates associated with the original dataset. The EOFs represent patterns of covariation in the spatial anomalies of soil moisture, and the ECs indicate the importance of each EOF to the pattern of anomalies on each date. By properly combining the spatial averages, the EOFs, and the ECs, the original soil moisture dataset can be completely reconstructed.

After the EOFs and the ECs are computed, statistically significant EOF/EC pairs to be retained in the downscaling method are determined. The statistical tests proposed by Bartlett (1950) and Johnson and Wichern (2002) were performed using 95% confidence levels. It was found that the Johnson and Wichern (2002) test tends to be overly restrictive in its estimate of the number of important EOFs, and the Bartlett (1950) test tends to be inaccurate with larger sample sizes (Perry and Niemann, 2007). Therefore, the results from the two tests were averaged to determine the final number of EOFs to be retained.

Next, multiple linear regression is used to identify empirical relationships between various topographic attributes and the retained EOFs. The topographic attributes are obtained from the DEMs of the application regions. Slope, aspect, and specific contributing area (SCA) are calculated using the methods described by Tarboton et al. (2009) to determine flow directions. With this information, other attributes are calculated including the cosine of the aspect (cosAspect), the natural log of SCA (lnSCA), the potential solar radiation index (PSRI), and the wetness index, which is lnSCA divided by the slope (Beven and Kirkby 1979). The PSRI value represents the ratio of the potential insolation received by a point with a given slope and aspect to that of a horizontal surface at the same location (Moore *et al*. 1993). The profile curvature, plan curvature, Laplace curvature, and tangent curvature are also calculated. Slope, SCA, lnSCA, wetness index and the curvatures are expected to be related to the lateral redistribution of soil moisture, while cosAspect and PSRI are expected to relate to spatial variations in evapotranspiration (Western *et al*., 1999). All of these attributes are standardized and regressed against each retained EOF. Stepwise multiple linear regressions are used to relate the significant attributes to the EOFs. Not all of the attributes are necessarily used in the final empirical equation.

Finally, piecewise-linear relationships are used, in place of the cosine function utilized by Perry and Niemann (2007), to estimate the retained ECs from the spatial-averaged soil moisture. The segmented linear relationship ensures that the EC is zero when the spatial average is at specified upper and lower bounds. These bounds disallow spatial variability once the spatial average soil moisture reaches the bounds. After conducting a sensitivity analysis, the lower and upper bounds were set to 0.04 and 0.56, respectively. Once this final task is complete, the EOF-based downscaling method is fully constructed. A fine-resolution DEM can now be used to determine topographic attributes, regression equations can estimate the EOFs from the attributes, the ECs can be estimated from a required spatial-average soil moisture value, and the computed EOFs, ECs, and the spatial average can be combined to determine the downscaled soil moisture pattern of any region and date assuming that the identified empirical relationships hold for the application conditions.

3.2 Non-linear Relationships

The nonlinear estimation methods examined are a spatial artificial neural network (SANN) and mixture modeling (MM) with multivariate Gaussian distribution functions. These methods were selected because they are unsupervised machine learning techniques that do not assume any specific form of relationship between soil moisture and the predictor data. Both are kernel density estimation methods, which attempt to estimate the joint probability density function between soil moisture and the predictor variables. Additionally, Green et al. (2007) found good performance when applying the SANN to crop yields, which are closely related to soil moisture. The nonlinear methods and MLR were used to estimate soil moisture patterns at three different study catchments to test the methods' predictive abilities when different processes dominate the construction of the soil moisture patterns. The catchments included the Tarrawarra, Satellite Station, and Cache la Poudre catchments.

The SANN method was developed by Shin and Salas (2000) and can be viewed as a specific implementation of the Nadaraya-Watson model, or kernel regression (Nadaraya 1964; Watson 1964; Bishop 2006). The method is similar to kernel density estimation using multivariate Gaussian kernels. The SANN method has two parameters: the number of neighbors P and the factor F. The parameter P relates directly to the kernel widths, and the effects of P on the individual kernel widths depend on the data configuration and density. The F parameter is related inversely to the kernel widths and affects all kernels to the same degree. For the research done by Coleman and Niemann (2012), the value of F is fixed at 2.5, and P is considered a free parameter and various values were tested. A disadvantage to the SANN method is that it requires all of the observations to be stored in order to make future estimates, which makes the evaluation slow for large datasets.

The MM method is similar to the SANN method in that estimates are made by conditioning a multivariate density function with the values of the predictor variables. However, the MM method uses the expectation-maximization (EM) algorithm (Dempster et al. 1977;

McLachlan and Peel 2000), and it uses a number of kernel functions that are less than the number of observations. As was previously mentioned, Gaussian functions are used as the kernel functions in the MM method. The MM method requires only one parameter, K, which is the number of components (Gaussian functions) used in the model. The parameter was varied from 1 to 4.

A Monte Carlo cross-validation methodology was utilized (McLachlan & Peel 2000; Bishop 2006) to assess the effectiveness of the estimation methods. The methodology divides each set of observations into training and testing sets. For each training set, the observations at unsampled locations comprise the testing set. Each of the three estimation methods was used to develop a model of the relationship between topographic attributes and soil moisture values based on the training sets. Soil moisture was then estimated at all locations with the models that were developed from each of the specific training sets. Finally, the Nash-Sutcliffe Coefficient of Efficiency (NSCE) (Nash & Sutcliffe 1970) was used to measure the model performance, but only the testing sets from the three estimation methods were used to calculate the NSCE.

3.3 The EMT Model

A detailed derivation and description of the EMT model is provided by Coleman and Niemann (2013). In short, the EMT model is a conceptual model derived to simulate physical processes that occur in the vadose zone of the soil. Four processes are included in the model to simulate the water balance of the vadose zone: infiltration F, deep drainage or recharge to groundwater G, lateral flow L, and evapotranspiration E. The water balance is assumed to be at equilibrium, thus disallowing hysteresis in the soil moisture patterns. The physical processes are represented in the model as functions of topographic attributes, which are determined from DEM grid cells. The topographic attributes derived from the DEM include slope, curvature as defined by Heimsath et al. (1999), SCA, and the PSRI on the summer solstice (Dingman, 2002).

Before applying the model, eleven soil, vegetation, and climatic parameters must first be calibrated using point soil moisture observations from the catchment. The calibrated parameter values were determined by maximizing the average NSCE for all of the dates in the available soil moisture dataset. After calibrations are completed, the EMT model can estimate fine-resolution soil moisture patterns in the catchments (Tarrawarra, Satellite Station, and Cache la Poudre) from a provided spatial-average soil moisture and topographic attributes. The model is designed to generate soil moisture values (θ) for each location within the catchment at the resolution of the input DEM (e.g. 15 m by 15 m). In order to obtain solutions for θ, a procedure is used to determine the weighted average solutions when evaluating the four processes of the vadose zone. Using the respective weights for each process, a final equation can be written to estimate the local soil moisture as a function of the spatial-average soil moisture and various climate, soil, and vegetation parameters that were assumed to be catchment-wide constants.

3.4 Sampling Techniques

The conditioned Latin hypercube sampling (cLHS) method proposed by Minasny and McBratney (2006) and a stratified random sampling (SRS) method similar to the SRS technique used by McKenzie and Ryan (1999) are the two strategic sampling techniques that were evaluated. The objective of both methods is to identify sampling locations that represent a diverse set of values for the ancillary variables so that the sampling is less likely to be redundant (Werbylo and Niemann 2014). The two methods are similar in that they select observation locations from locations that are divided into bins. The methods differ, however, in how they determine the composition of the bins. The cLHS method divides the range of each ancillary variable into equally probable bins such that each bin contains the same number of observations. The SRS method divides the range of each ancillary variable into bins that cover an equal fraction of the observed range, regardless of the number of observations within each bin. Figure 1 demonstrates how the binning of the sampling techniques would look for a hypothetical relationship between an ancillary variable and soil moisture.

The sampling methods were used with the two downscaling models described earlier: the EOF method from Busch et al. (2012) and the EMT model from Coleman and Niemann (2013). The sampling techniques used the topographic attributes to identify locations where the soil moisture should be monitored, and then the recorded soil moisture values were used to define the relationships required by the downscaling methods.

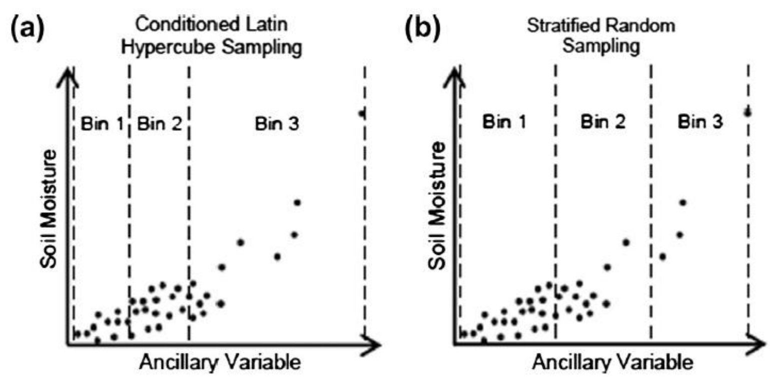

Figure 1. Application of the cLHS and SRS binning methods for a hypothetical relationship between an ancillary variable and soil moisture.

The performance of the sampling techniques was determined by the ability of the downscaling methods to reproduce the actual catchment-scale soil moisture patterns at the application sites (Tarrawarra, Satellite Station, and Cache la Poudre) when supplied with data from the sampling methods. In the study that was conducted, the sampling methods were compared to random sampling, which was used as the control case. This approach was taken because it is similar to other studies that have evaluated the effectiveness of strategic sampling methods (Minasny and

McBratney 2006; Worsham et al. 2012). Additionally, random sampling was selected because the number of sampling locations could be controlled more directly (compared to uniform sampling, for example).

3.5 Effects of Vegetation

To evaluate the role of vegetation, soil moisture was monitored at intercanopy locations, under the shrub canopy, and under the forest canopy on both the north-facing and south-facing hillslopes of the Cache la Poudre catchment. Mountain mahogany shrubs and ponderosa pine trees are some of the dominant species that vegetate the region, and thus they were used to evaluate the effects of a shrub canopy and a forest canopy, respectively. Soil moisture was also monitored at different upslope and downslope distances from plant bases, attempting to evaluate the importance of stemflow and run-on effects. Soil moisture observations were collected on an hourly basis using time-domain reflectometry (TDR). Rain gauges were also placed at the various locations in order to measure throughfall. Temperature and insolation measurements were collected to determine the potential evapotranspiration (PET), which was calculated for each location type using the Priestly and Taylor (1972) equation. Observations of soil texture and the degree of hydrophobicity were also taken. Sieving was used to remove any gravel and to collect the sand (0.05-2 mm) fraction of the soil. The silt (0.02-0.6 mm) and clay (<0.02 mm) fractions were determined using a hydrometer. The degree of hydrophobicity of the soil samples was determined by using the molarity of ethanol droplet (MED) test (Roy and McGill 2002).

Using the south-facing slope's (SFS) intercanopy locations as the base condition (condition with the least possibility of having effects from vegetation), the measurements were compared and the effects of vegetation on shallow soil moisture were assessed. Sensors on the SFS and NFS have labels that begin with 'S' and 'N', respectively. The three canopy locations;

intercanopy, mountain mahogany canopy, and ponderosa pine canopy, are labelled ‘I’, ‘M’, and ‘P’, respectively. Therefore, the six primary location types are labelled SI, SM, SP, NI, NM, and NP. Also, at one site on the SFS, throughfall and insolation were measured above the canopy, which was considered an open site and was labelled SO.

3.6 The EMT+VS Model

Similar to the EMT model, the vadose zone of the soil was simulated by the EMT+VS model. In the EMT+VS model, a water balance is again constructed to consider infiltration F, deep drainage G, evapotranspiration E, and lateral flow L. In this case, however, the processes are modified to also include the roles of interception, transpiration, and soil evaporation.

Interception by vegetation modifies the infiltration term. The adjustment allows for the fact that interception would cause a decrease in infiltration. The ET process is also modified because the EMT model does not distinguish transpiration and evaporation due to effects of vegetation. By introducing a fractional vegetation cover (V), the EMT+VS model accounts for both evaporation and transpiration. The vegetation cover is applied to the transpiration term to show that denser vegetation cover is associated with increases in transpiration. It is also applied to soil evaporation to show that soil evaporation is reduced by denser vegetation cover.

In addition to the process modifications, the structure of the model was revised to allow both vegetation and soil data to vary at fine-resolutions. Nonetheless, the EMT+VS model uses a weighted average solution strategy that is used for the EMT model. The only difference is that more variables are allowed to vary spatially in the EMT+VS model.

The model was evaluated by applying it to the Cache la Poudre catchment, where fine-resolution topographic and soil moisture data were available on a 15 m grid. Vegetation data were measured on the 15 m grid, and soil data were collected at alternating points from the 15 m grid, producing a 30 m grid. It was also tested at the Tarrawarra and Nerrigundah catchments in Australia where soil moisture, topographic, and limited soil data were available. Because the soil data at the Australian catchments are limited, the feasibility of interpolating soil data for use with the EMT+VS model was also evaluated.

4. Application Sites

4.1 Tarrawarra

The Tarrawarra catchment is located near Melbourne in southern Victoria, Australia (Western and Grayson 1998). It has a temperate climate with an annual precipitation of approximately 82 cm, an annual PET of approximately 83 cm, and a rainfall deficit in summer and excess in winter. The vegetation of the catchment consists primarily of grassy pasture used for cattle grazing. The soils generally consist of a silty loam A horizon over a clay B horizon, and the soil depths vary from 40 cm in the upper catchment to over 2 m in the lower region. The catchment area is 10.5 ha, and the topography consists of undulating hills with topographic relief of 27 m. A DEM with 5 m resolution is available for the site, which was created by interpolating elevations that were collected using a total station on a paced 10 m grid. Soil moisture data were collected at Tarrawarra on 13 dates between September 27, 1995 and November 29, 1996 on a 10 x 20 m sampling grid using a portable TDR. The soil moisture was measured in the top 30 cm of the soil layer. The soil moisture dataset was filtered to include only those locations that were observed on all dates, resulting in a dataset with 454 locations.

4.2 Tarrawarra 2

The Tarrawarra 2 catchment surrounds the original Tarrawarra catchment and is described by Wilson et al. (2005). The catchment exhibits similar characteristics to the Tarrawarra catchment including climate, precipitation, PET, vegetation, and soil type. The catchment has an area of approximately 115 ha with topographic relief of 41 m. The available DEM for the catchment has a 10 m resolution. Soil moisture data were collected at Tarrawarra 2 on eight dates between June 1998 and October 1999, a few years after the dataset for Tarrawarra was collected. The data at Tarrawarra 2 were also collected using a portable TDR on a 40 x 40 m grid. After filtering the data, the soil moisture dataset includes 374 locations. It should be noted that the Tarrawarra dataset was collected during a wetter than average period while the Tarrawarra 2 dataset was collected during a drier than average period. Nonetheless, the soil moisture patterns at the two catchments are expected to exhibit similar behavior.

4.3 Cache la Poudre

The Cache la Poudre catchment is near Rustic, Colorado and approximately 40 km west of Fort Collins, Colorado (Lehman and Niemann 2008). The catchment has a semiarid climate where annual precipitation is approximately 40 cm and annual PET is approximately 93 cm. It is substantially drier than the Tarrawarra and Tarrawarra 2 catchments. The vegetation on the north-facing slope of the catchment is predominately coniferous forest with scattered shrubs, whereas the south-facing hillslope is primarily covered with shrubs and grasses. The catchment has thin sandy soil on the south-facing hillslope and thicker mineral soils overlaid with organic matter on the north-facing hillslope. The Cache la Poudre catchment has an area of 8 ha with topographic relief of 115 m, and it consists of the headwater area for one incised channel with both steep and flat portions. The DEM for the catchment was created by surveying on a 15 m grid. Soil moisture data were collected on nine dates over a period of three months from April to June 2008. A portable TDR was used to collect the measurements, but because of the shallowness of the soils in this catchment, the soil moisture was only measured in the top 5cm of the soil. The soil moisture data were collected on the same 15 x 15 m grid as the DEM. After filtering to produce a consistent dataset, a total of 347 locations remain.

4.4 Satellite Station

The Satellite Station catchment is located approximately 70 km north of Aukland, New Zealand, and is described by Wilson et al. (2003). The catchment has a humid climate where annual precipitation is approximately 160 cm and annual PET is approximately 130 cm. Consequently, Satellite Station is the wettest catchment that was evaluated during this research. The catchment is used for cattle grazing, and the soil characteristics have a clear distinction between the hillslopes and the lowland valleys. Hillslope soils are generally silty clay loam with 30 cm depths, while the lowland valley soils are relatively deep alluvial fills with high clay content. The area of the catchment is approximately 60 ha and comprised of undulating terrain with a total relief of 80 m. The topographic data for the catchment are available as a 10 m resolution DEM. Soil moisture data were collected at Satellite Station on six dates from March 1998 to October 1999. These measurements were made on a 40 x 40 m grid using a portable TDR device to measure soil moisture to a depth of 30 cm. Again, the dataset was filtered, resulting in a dataset with 322 locations.

4.5 Nerrigundah

The 6 ha Nerrigundah catchment is located northwest of Dungog in New South Wales, Australia (Walker 1999; Walker et al. 2001). It has a temperate climate where annual precipitation is approximately 100 cm and annual PET is approximately 160 cm. Natural grasses vegetate the catchment where soils are usually shallow (30-90 cm) predominantly consisting of sandy loams. The catchment has an average elevation of approximately 110 m with topographic relief of 27 m. A total station survey was conducted to develop the available 20 m DEM. Soil moisture data were collected for the top 15 cm of the soil on 12 dates from August 27, 1997 to September 22, 1997. A TDR was used to measure the soil moisture within the catchment on a 20 x 20 m grid. The soil moisture dataset was filtered and produced a dataset with 238 locations.

5. Results

5.1 The EOF Method

Figure 2 displays the significant EOFs for the four analyzed catchments. For Tarrawarra, the Bartlett (1950) test indicates that five EOFs are significant, whereas the Johnson and Wichern (2002) test identifies only one as significant. Therefore, three EOFs are retained in the downscaling method. The three EOFs explain 54.9%, 9.4% and 5.9% of the variation in the Tarrawarra dataset, respectively, for a total of 70.2 %. The Bartlett (1950) test indicates that three EOFs are significant and the Johnson and Wichern (2002) test indicates one EOF as significant for the Tarrawarra 2 dataset, resulting in two EOFs being retained in the downscaling method. The two EOFs explain 25.3% and 15.9% of the variation, respectively, for a total of 41.2%. At Cache la Poudre, the statistical tests produced similar results to the Tarrawarra 2 dataset, resulting in the first two EOFs being retained in the downscaling method. The EOFs explain 50.2% and 13.9% of the variation, respectively, for a total of 64.2%. For Satellite Station, both statistical test methods indicate that only one EOF is significant, and it explains 29.8% of the variation in the dataset.

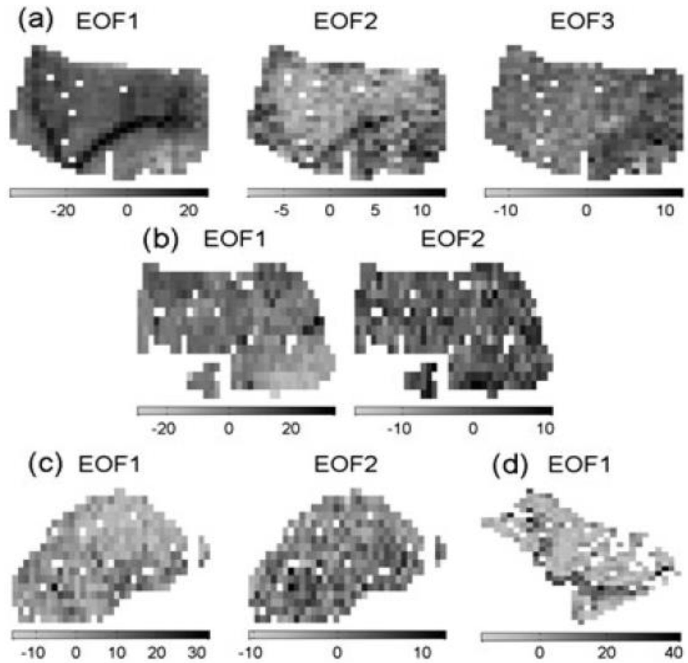

Figure 2. Retained EOFs for (a) Tarrawarra, (b) Tarrawarra 2, (c) Cache la Poudre and (d) Satellite Station. White cells indicate locations that were excluded from the EOF analysis because soil moisture observations were missing in the original dataset

As was described previously, multiple linear regressions were used to identify empirical relationships between various topographic attributes and the retained EOFs. The EOF patterns that were estimated using the regression equations are denoted as REOFs and are presented in Figure 3. When comparing the REOFs (Figure 3) with the actual EOFs (Figure 2), it can be seen that the REOFs are reasonably similar to the EOFs, but they appear to be smoother. For Tarrawarra, the portion of the variation in each EOF that is explained by the corresponding REOF is 0.72 for EOF1, 0.39 for EOF2 and 0.22 for EOF3. For Tarrawarra 2, the portion of variation explained is 0.41 for EOF1 and 0.09 for EOF2. The portions are 0.26 for EOF1 and 0.13 for EOF2 for the Cache la Poudre catchment, and for Satellite Station, the amount of variation explained within EOF1 by the empirical relationships is 0.38.

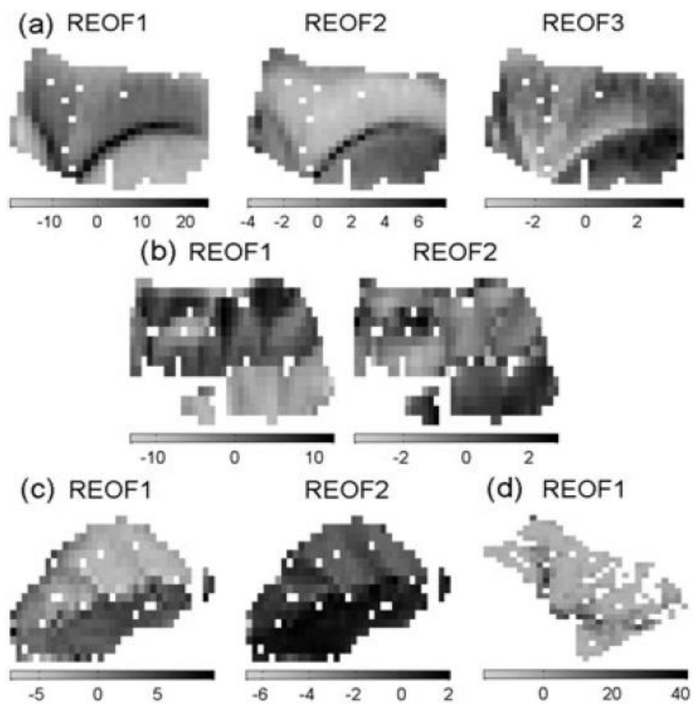

Figure 3. EOFs estimated based on the regressions against topographic attributes for (a) Tarrawarra, (b) Tarrawarra 2, (c) Cache la Poudre and (d) Satellite Station. White cells indicate locations with no values in the original soil moisture dataset

Overall, it can be seen that the topographic attributes are more successful at explaining the most important EOFs at each catchment. Tarrawarra's EOFs are most strongly related to the topographic attributes, whereas Cache la Poudre's EOFs are most weakly related. The weaker relation is likely attributed to the drier conditions and shallow measurement depths at the Cache la Poudre catchment.

The EOFs are used to produce downscaled soil moisture patterns in combination with the retained and estimated ECs. The downscaling method was applied to each catchment in four ways. First, each downscaling method was applied when the actual EOFs and ECs were used. Second, the actual EOFs and the estimated ECs were used. Third, the method used the estimated EOFs and the actual ECs. Fourth, the estimated EOFs and the estimated ECs were used. This approach was executed to better understand the origins of the errors that occurred in the downscaled patterns. The NSCE was used to measure the difference between the observed and the downscaled soil moisture patterns. The maximum value of NSCE is one, which implies that the downscaled pattern matches the observed pattern exactly. NSCE values greater than zero indicate the downscaled pattern explains more of the observed variability than does simply using the spatial average soil moisture.

Figure 4 shows the results of the analysis. The average NSCE values are the highest when the actual EOFs and ECs are used. The only reason why the NSCE values are not equal to one in this case was because of the discarded EOF/EC pairs that were not retained for the downscaling method. When the analysis was repeated using the estimated ECs in place of the actual ECs, the average NSCE values decrease further. Using this information is essentially what was done be Perry and Niemann (2007) who downscaled soil moisture patterns by using a space-time dataset of soil moisture and a spatial-average soil moisture value. The error that is introduced by estimating the patterns of covariation from the topographic attributes can be realized by looking at the analysis that uses the REOFs and actual ECs.

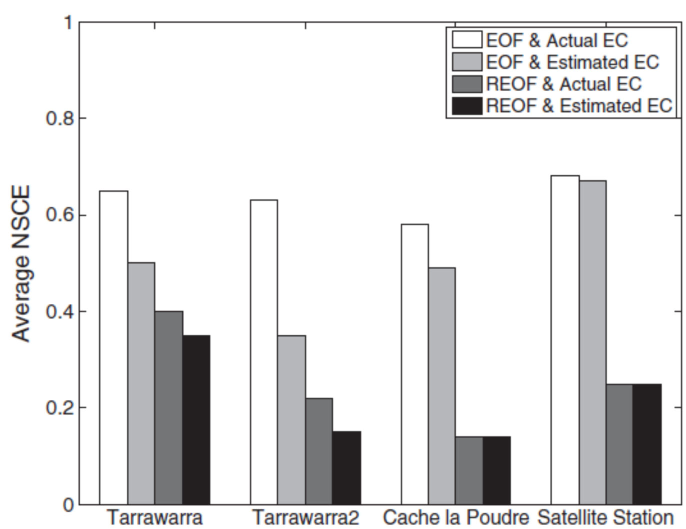

Figure 4. Performance of the downscaling method at each catchment as the estimated ECs and EOFs replace the actual ECs and EOFs in the method. In the legend, 'EOF' indicates that the downscaling method used that actual EOF, and 'REOF' indicates that the method used the estimates obtained from the topography. Similarly, 'actual EC' means that the method used the EC values obtained from the EOF analysis, whereas 'estimated EC' means that the method used the estimates obtained from the spatial-average soil moisture

In this case, one can see the topographic dependence that the catchments possess. Tarrawarra's soil moisture patterns contain the strongest relationship to the topographical attributes because the NSCE drops from 0.63 to only 0.40, whereas Cache la Poudre exhibit the weakest relationship because the NSCE drops from 0.58 to 0.14. Overall, the figure demonstrates that the primary source of error in the downscaling method results from the estimation of the EOFs from topographic data. Thus it suggests that the use of additional data such as soil and vegetation variations might represent a way to improve the downscaling method. As expected, the lowest NSCE values are achieved when both the EOFs and the ECs are estimated. However, the fact that the NSCE values are positive indicates that the downscaling method produces a soil moisture pattern that is better than using just the spatial average soil moisture. The advantage of this final method is that it can possibly be used for other similar catchments where no space-time soil moisture observations have been collected.

Figure 5 illustrates the best performance of the downscaling method at each catchment. The NSCE values for these patterns are 0.67 for Tarrawarra, 0.35 for Tarrawarra 2, 0.33 for Cache la Poudre and 0.34 for Satellite Station. From the figure, it can be seen that the downscaling method successfully captures most of the major features of the observed patterns at all four catchments. At Tarrawarra, the downscaled pattern successfully identifies the wet valley bottom, and it identifies the relatively drier soil moisture on the north-facing slope. At Cache la Poudre, the downscaled pattern produces relatively wetter locations on the north-facing hillslope, which is consistent with the observed pattern. All of the estimated patterns are much smoother in appearance than the observed patterns because the REOFs are much smoother than the actual EOFs.

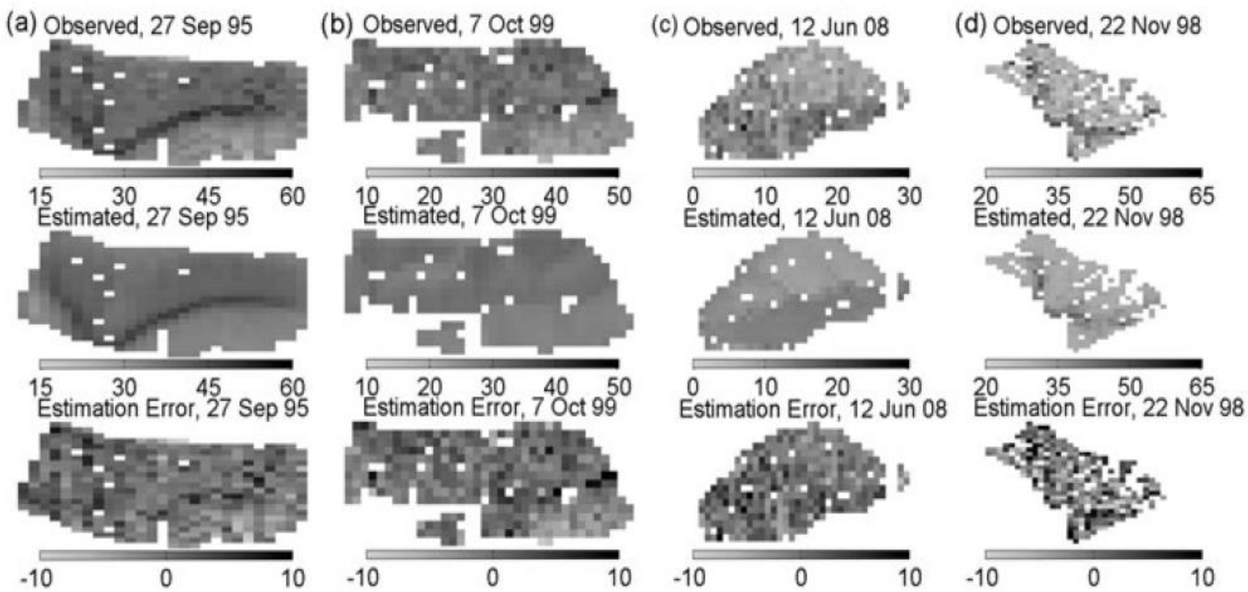

Figure 5. Comparisons of observed soil moisture patterns and those estimated by the EOF-based downscaling method at (a) Tarrawarra, (b) Tarrawarra 2, (c) Cache la Poudre and (d) Satellite Station. These dates were selected because their NCSE values are the highest among all dates at the given catchment. Soil Moisture values are volumetric soil moisture expressed as a percentage. White cells indicate locations with no values

The probability of the EOF-based downscaling method was then evaluated. In the analysis, the downscaling method that was developed at each catchment was applied to the other three catchments. When applied to the other catchments, the performance of the methods is almost always worse. The generally poor transferability of the methods between the datasets could be attributed to a number of causes including: differences in precipitation during times of data collection, differences in DEM resolutions, the number of attributes associated with the respective REOFs, and the fact that the REOFs are estimated on the basis of topography alone while neglecting consideration of soil and vegetation properties.

5.2 Non-linear Relationships

The observed soil moisture patterns and the patterns estimated when 25% of the available data were used for training for the three application regions are shown in Figure 6. The patterns

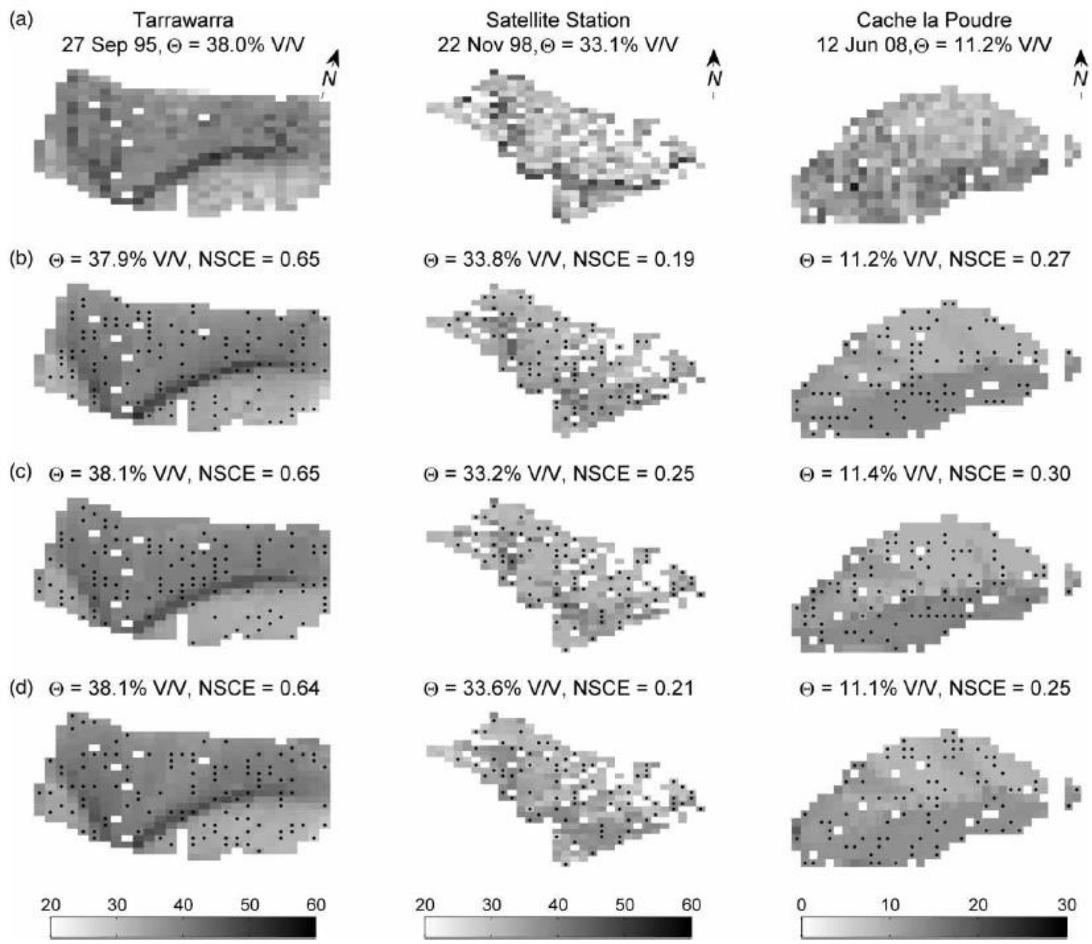

Figure 6. (a) Observed soil moisture patterns at each study site, and soil moisture patterns estimated by (b) MLR, (c) SANN and (d) MM. The dots indicate training data locations.

shown are from the set of topographic attributes that produced the highest median NSCE for each method and the training data that produced the results closest to that median NSCE among different samples. The main features observed in the soil moisture patterns are reproduced by all of the methods. The wet valley bottom and south-facing hillslope of the Tarrawarra catchment are reproduced by each of the methods. Satellite Station has a weakly organized soil moisture pattern, but the methods are able to capture some of the variability. The methods are also able to reproduce the mostly aspect-dependent pattern of the Cache la Poudre catchment, which distinguishes the soil moisture of the south-facing hillslope and the north-facing hillslope. The NSCE values included in the figure were calculated only from the associated testing dataset. The methods generally perform better at Tarrawarra compared to the other two sites, but the SANN has the highest NSCE value for all three application catchments. The SANN method most likely performs better than the other two methods because it has the most flexibility in the type of relationship that it can infer from the data. The flexibility allows the SANN to include intricacies in the relationships to the topographic attributes that are ignored by the other two methods.

Figure 7 plots the median NSCE for the three methods as the number of topographic attributes used varies. For each application site, the driest, wettest, and a moderate wetness condition were evaluated. In all cases, 25% of the observations were used as training data, and the lines in the figures indicate the median NSCE values from all 30 samples at that sampling rate. In nearly all of the scenarios, the performance of the three estimation methods is similar. The largest notable difference between performances can be seen at Satellite Station for both the dry and moderate wetness conditions. In both cases, the SANN method has the best performance. Although it is not as noticeable, the SANN performs better than the other methods in most of the other cases in the figure as well. In general, the methods perform better under the moderate wetness condition. The reduced performance in the dry and wet conditions could be expected because of the reduced spatial structure of the soil moisture patterns during those conditions.

The overall similarity of the results of the MLR, MM and SANN estimation methods indicate that allowing nonlinearity in the relationships between soil moisture and topographic attributes does not substantially improve pattern estimation. For most of the cases in the figure, the methods show little variation in the NSCE as the number of predictor variables is increased.

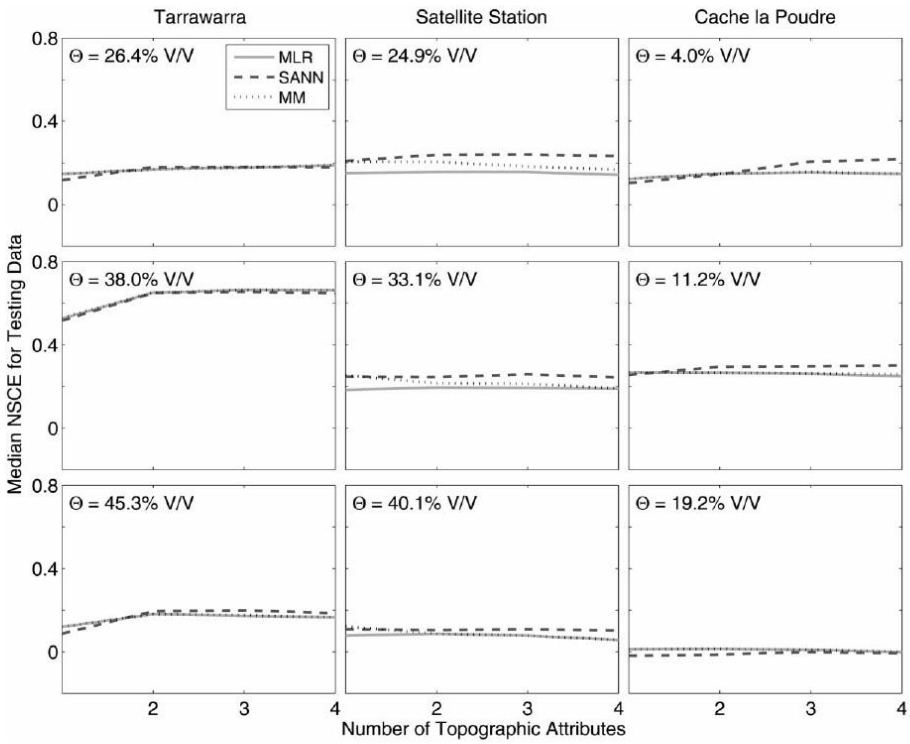

Figure 7. Median NSCE for each estimation method as the number of topographic attributes used increases.

The exceptions are the moderate and wet conditions at Tarrawarra and the dry condition at Cache la Poudre. Overall, the NSCE for the SANN method usually remain somewhat constant or improve with additional predictor variables, while the other two methods generally decrease with additional variables. The lack of substantial improvement with additional variables suggests that one or two attributes represent the major effects of the dominant physical processes. The negative trends in NSCE values as predictor variables increase indicate overtraining.

The effects of the size of the training dataset on the performance of the methods are illustrated in Figure 8. The figure shows the results associated with the maximum median NSCE value produced by the use of two predictor variables. Only the moderate wetness condition is shown for each site, but the results are consistent for all three wetness conditions. The plots in the figure characterize the variation in the performance of each method among the 30 training

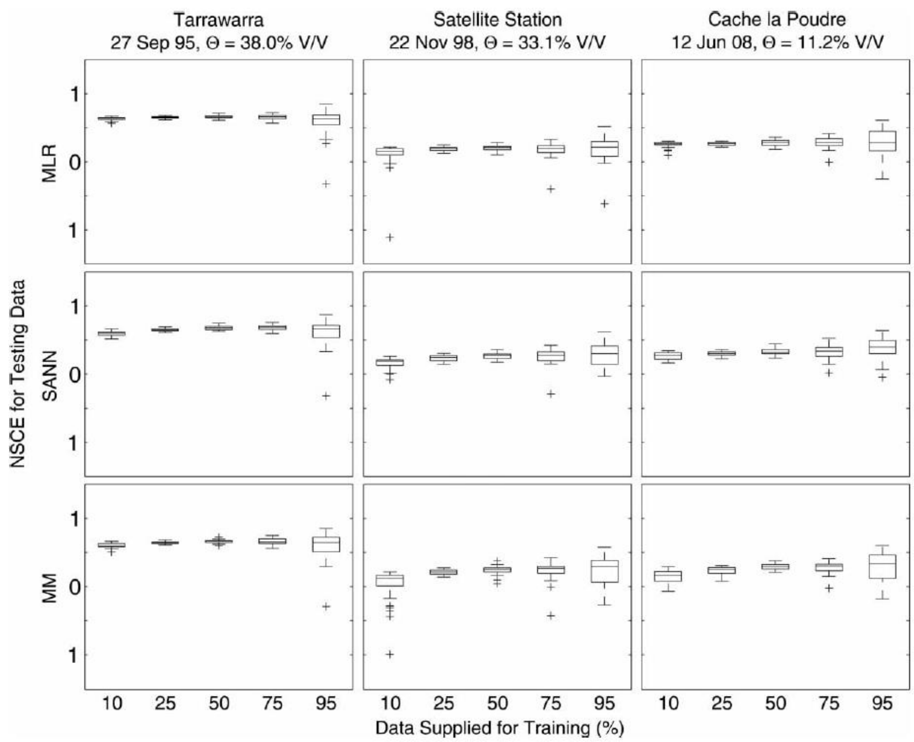

Figure 8. Box-and-whisker plots characterizing the performance of each estimation method as the amount of training data increases. Plus symbols indicate outliers, which are defined as values that are more than 1.5 times the distance between the upper and lower quartiles away from the box limits.

sets generated at a given sampling density. In general, the performance is not significantly influenced by the number of observations supplied for training. In some cases, the performance slightly decreases, and in other cases it slightly increases as the sampling rate is increased. Overall, the nonlinear methods' best performances are obtained by using more data than the MLR, which demonstrates the nonlinear methods' abilities to continue to extract useful information as the amount of data increases. However, at least 50% of the data supplied for training has to be used to achieve the best performance for all of the estimation methods. This indicates that a significant data collection effort would be required. In light of that fact, the 10 and 25% sampling rates are more aptly evaluated. These rates are associated with a much more feasible manual collection effort. At those sampling rates, the SANN has the highest median NSCE at Satellite Station and Cache la Poudre, and MLR has the highest value for Tarrawarra.

For the most part, the SANN obtains equivalent or higher NSCE values than MLR when the sampling rate is at least 25%. Additionally, the MM outperforms MLR in most cases when the sampling rate is at least 50%.

5.3 The EMT Model

Realistic soil moisture patterns can be produced by assuming that the spatial structure of the patterns is at equilibrium and by inferring the spatial variability of the physical processes from topographic attributes (Coleman and Niemann, 2013). Separate calibrations were performed for each of the three catchments seeking the maximum average NSCE for all the dates in the available soil moisture dataset. At the Tarrawarra catchment, shown in Figure 9, the EMT model shows increasingly prominent wet areas in the valley bottoms as the spatial-average soil moisture increases from (d) to (f). In contrast, the hillslope dependence decreases as spatial-average soil moisture increases. The model seems to slightly overestimate the valley bottom dependence for this catchment. However, the overall topographic dependencies for Tarrawarra are successfully reproduced.

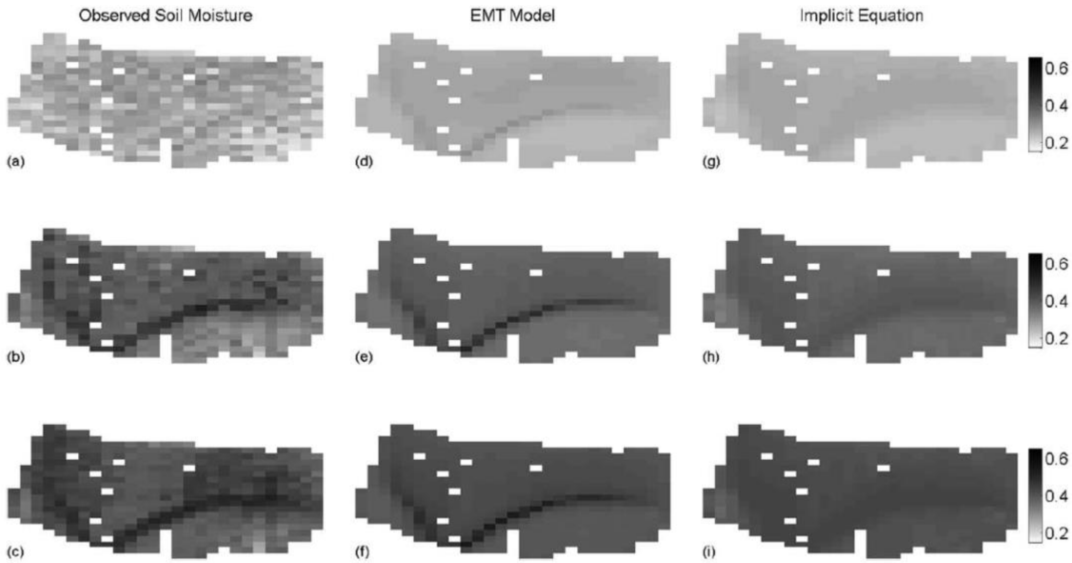

Figure 9. Representative observed (a, b, c), EMT model (d, e, f), and implicit equation (g, h, i) soil moisture patterns for Tarrawarra. The observed soil moisture patterns are from 14 February 1996, 27 September

The estimated soil moisture patterns for Satellite Station (Figure 10) exhibit stable wet valley bottoms. This feature is likely due to lateral flow having a large effect on soil moisture. Overall, it can be seen that the estimated soil moisture pattern closely resembles the observed pattern, and it captures most of the observed scatter and variability.

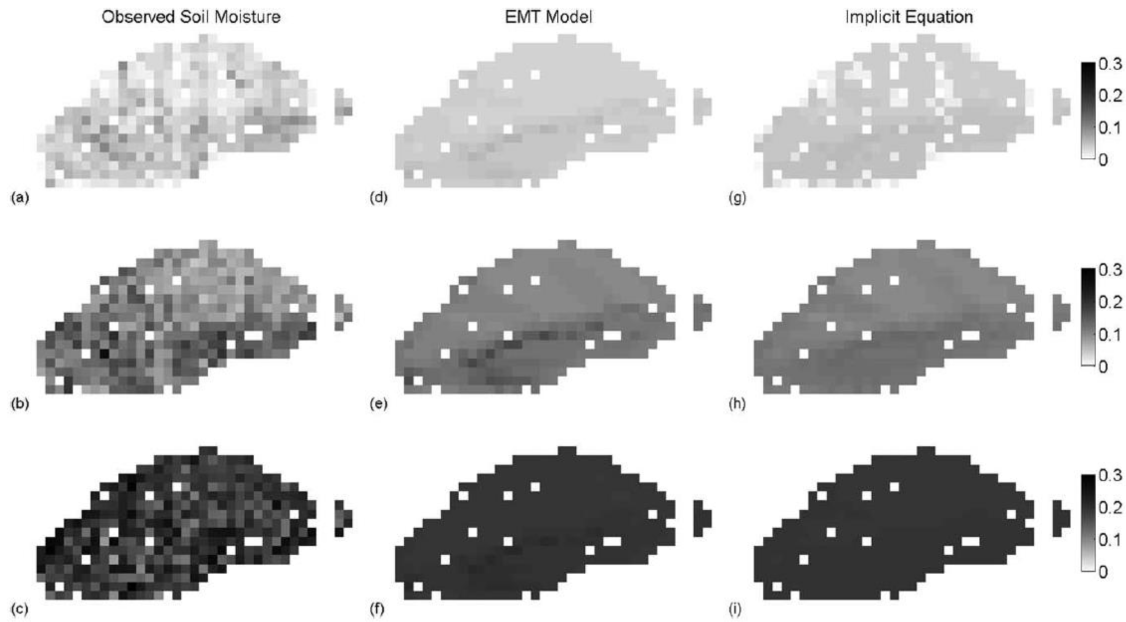

Figure 11. Representative observed (a, b, c), EMT model (d, e, f), and implicit equation (g, h, i) soil moisture patterns for Cache la Poudre. The observed soil moisture patterns are from 24 June 2008, 12 June 2008, and 28 May 2008, and the spatial-average soil moisture values are 0.04, 0.11, and 0.19 V/V for Figures 4a, 4b, and 4c, respectively. NSCE values for the EMT model are 0.10, 0.20, and 0.00.

The ranges of NSCE among the dates and catchments are shown in Table 1. On average, the model explains between 8% and 30% of the spatial variation in the soil moisture. The best performance occurs at Tarrawarra, where the model explains up to 58% of the variation on one particular date. These NSCE values are similar to the performance of other methods that estimate soil moisture based on topography at these sites (Coleman and Niemann, 2012; Perry and Niemann, 2007; Western et al., 1999; Wilson et al., 2005).

Table 1. Statistics of the NSCE Values from All Available Dates at the Three Catchments when the Best-Performing Parameter Sets are Used

	Tarrawarra	Satellite Station	Cache la Poudre
Maximum	0.58	0.27	0.20
Average	0.30	0.17	0.08
Minimum	0.05	0.09	−0.02

The relative importance of the two spatial patterns that are embedded in the EMT model (the lateral flow index (LFI) and the evapotranspiration index (ETI)) depend on the spatial-average soil moisture in the catchment. The relative weight for each term in the EMT model as a function of spacial-average soil moisture is plotted in Figure 12. For the Tarrawarra catchment (Figure 12a) at low spatial-average soil moistures, the radiative ET weight is largest, implying hillslope-dependent soil moisture patterns to be the most important. Conversely, as spatial-average soil moisture becomes large, the later flow weight and the influence of LFI are very large, producing valley-dependent soil moisture patterns. At Satellite Station (Figure 12b), aerodynamic ET and deep drainage dominate at the lower and upper ends of the spatial-average soil moisture range, respectively.

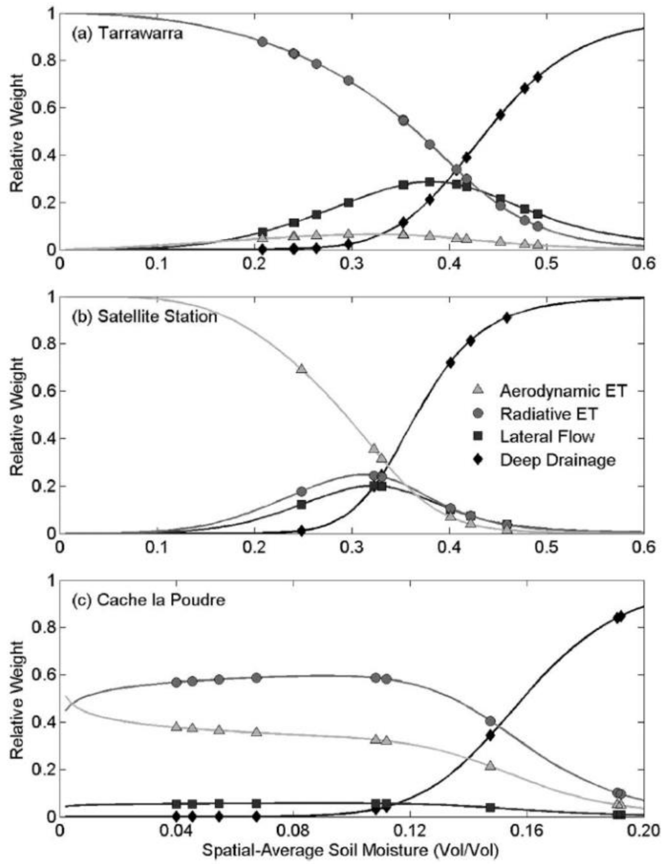

Figure 12. Calibrated weights plotted as a function of spatial-average soil moisture for (a) Tarrawarra, (b) Satellite Station, and (c) Cache la Poudre. Markers indicate observed spatial-average soil moisture values and the associated process weights.

Lateral flow is more important at Satellite Station than Tarrawarra, and the radiative ET weight is less important. For Cache la Poudre (Figure 12c), deep drainage processes dominate at the upper extreme of the range of spatial-average soil moisture, but it is already important for much lower soil moistures. The lateral flow weight is small for the entire range, which supports the lack of valley dependence in the soil moisture patterns of the Cache la Poudre catchment.

5.4 Sampling Techniques

The sampling techniques were evaluated for two scenarios: location-limited and date-limited. For the location-limited scenario, the sampling methods were used to select a limited number of locations in a catchment based on the topographic attributes that are required by each downscaling method as ancillary variables. For the date-limited scenario, all available locations were sampled but only on a limited number of dates. In this scenario, the spatial average soil moisture, which varies between different dates, was treated as an ancillary variable (the only ancillary variable). For any given number of sampling locations and/or dates, the selection of actual locations and dates was repeated numerous times to produce multiple realizations. The EOF method requires about 100 realizations for the average performance of the model to stabilize. The EMT model requires only about 50 trials because it has fewer ancillary variables (topographic attributes) and parameters.

Figure 13 presents the results for the location-limited scenario at the three application catchments when the spatial average soil moisture is estimated from the sampled locations. In general, cLHS consistently outperforms random sampling. When very few locations are sampled (fewer than about 30), SRS performs as good as or better than cLHS. This result is not seen at Cache la Poudre, and the difference can mostly be attributed to the fact that the catchment is hillslope-dependent and because the soil moisture patterns at Cache la Poudre are most weakly related to topography relative to the other two catchments. However, for large numbers of sampled locations, SRS can perform worse than both cLHS and even random sampling.

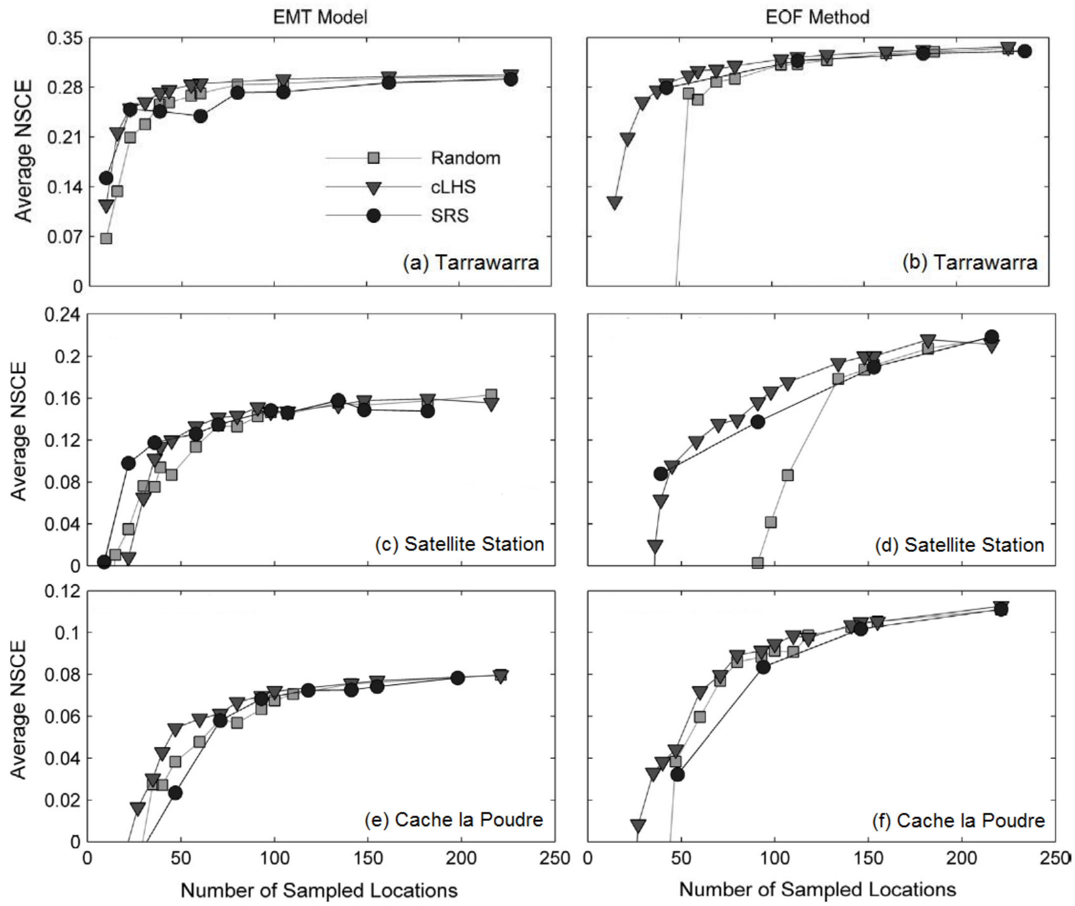

Figure 13. Average NSCE of the downscaling methods at Tarrawarra (top row), Satellite Station (middle row), and Cache la Poudre (bottom row) when the number of sampled locations and the sampling method are varied. The left column considers the EMT model, while the right column considers the EOF method.

Comparing the left column of results to the right column in Figure 13 allows a comparison of the EMT model and EOF method when they are calibrated with soil moisture observations from limited numbers of locations. The random sampling case allows for the most direct comparison because the same locations are used in both cases. The results show that the EMT model significantly outperforms the EOF method when smaller numbers of locations are used: less than 55 for Tarrawarra, less than 130 for Satellite Station, and less than 47 for Cache la Poudre. When the numbers of locations are large, the EOF method outperforms the EMT model. The EMT model likely performs better with limited data because it is based on a physical description of vadose-zone hydrology that helps constrain the estimated patterns. The EOF method likely performs better with large datasets because its empirical approach allows greater flexibility in reproducing the observed patterns.

In the date-limited scenario, the downscaling methods were calibrated using every soil moisture observation from the selected sampling dates. Then, the downscaling methods were used to estimate the soil moisture patterns on all available dates when supplied with the true spatial average. Figure 14 shows the results of the limited-date scenario when it is coupled with each of the downscaling methods and all three application sites. Overall, little improvement in performance occurs after three to four dates have been observed, depending on the sampling method used.

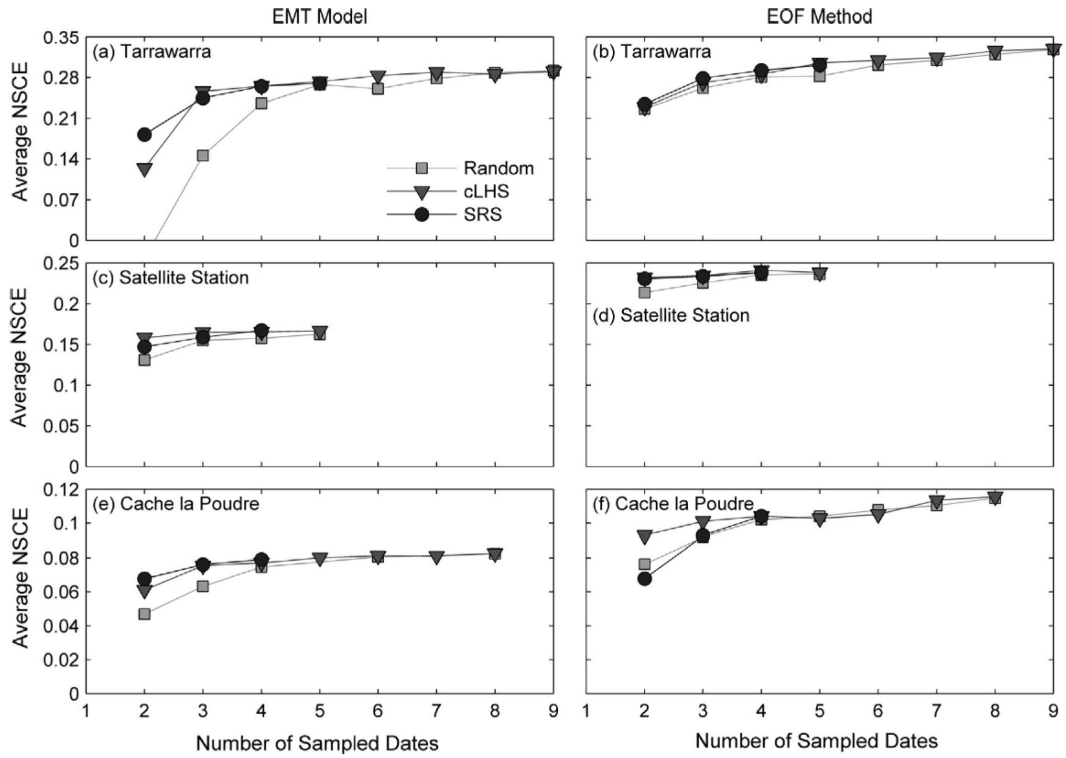

Figure 14. Average NSCE of the downscaling methods when the number of sampled dates and the sampling method are varied. The left column considers the EMT model, while the right column considers the EOF method. The top row considers Tarrawarra, the middle row considers Satellite Station, and the bottom row considers Cache la Poudre.

A large advantage is observed for strategic sampling at Tarrawarra when the EMT model is used (Figure 14a). The advantage is not as evident when applying the EOF method to Tarrawarra or when either downscaling method is applied to the other two application sites. The differences are likely smaller at the other catchments because the soil moisture patterns are temporally stable. When selecting dates at Tarrawarra, it is more important that dry, intermediate, and wet conditions are represented because the soil moisture patterns are different for each condition at that catchment. The strategic sampling methods ensure the inclusion of the varying conditions, and that is why they outperform random sampling so clearly in Figure 14a. It should be noted that the EOF method outperforms the EMT model in all cases of the date-limited scenario in part because all available locations are sampled on any selected date.

coefficients of variation to the NFS intercanopy case. The effect of vegetation cover differs between the two hillslopes because the intercanopy soil moisture differs (the behavior of the canopy locations was similar on both hillslopes). Compared with the SFS intercanopy case, the NFS intercanopy soil moisture is a little greater on average and exhibits less temporal variation with respect to its average. The difference between the two intercanopy cases mostly results from differences in the soil moisture values during dry periods.

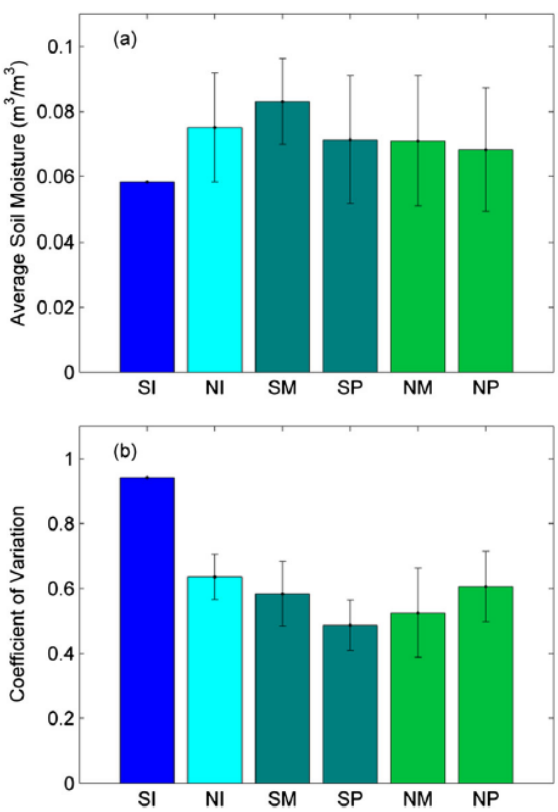

Figure 15. (a) Average and (b) coefficient of variation of soil moisture for all location types. For locations having more than one soil moisture probe (all but SI), the plotted values are the averages amongst all probes for that location type. The error bars show the standard deviation of the average and coefficient of variation for each soil type.

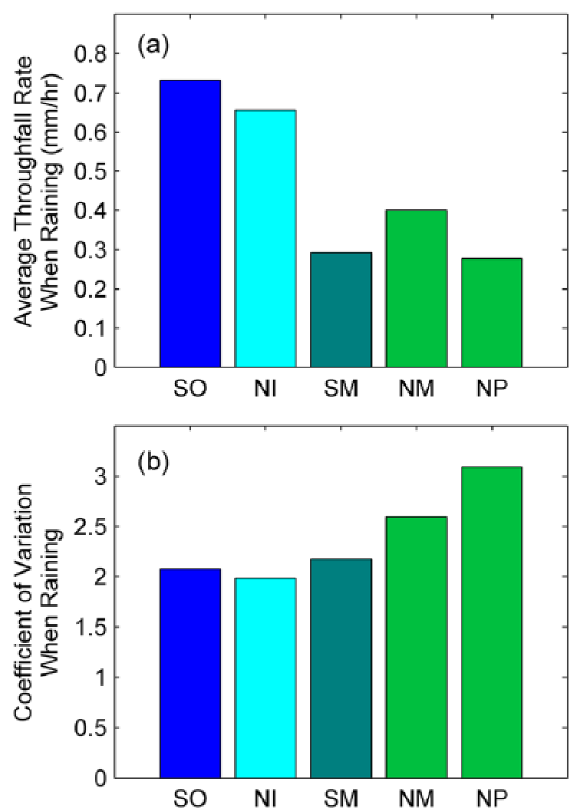

Figure 16. (a) Average and (b) coefficient of variation of hourly throughfall rate for the available location types. This analysis excludes periods when no throughfall or precipitation was recorded at any gauge. Averages are low in part because the calculation can include zeroes if rainfall or throughfall was recorded at other gauges.

The second objective was to understand why vegetation has the observed effects on the shallow soil moisture. It was hypothesized that differences in interception help produce the observed differences in soil moisture, and the results (Figure 16) support this hypothesis. The throughfall rates under both canopy types are typically much smaller than the rainfall rates in the open. Interception helps explain why the soil is typically drier under the canopy types during wet periods, which are associated with rainfall events. Throughfall for the NFS intercanopy case is similar to rainfall in the open. This result helps explain why its soil moisture is similar during wet periods to the SFS intercanopy location, which is also expected to experience little interception.

It was also hypothesized that differences in shading contribute to the observed differences in shallow soil moisture. This hypothesis was also supported by the results as shown in Figure 17. Shading from both canopy types produces substantially lower PET under the vegetation cover than in the open. Shading is expected to reduce soil evaporation and preserve the soil moisture under the canopy. Thus, it helps explain why the soils are wetter for canopy locations than intercanopy locations during dry periods. The NFS intercanopy location also experiences substantial shading from the nearby canopy, whereas SFS intercanopy locations are unlikely to experience much shading because the shrubs are shorter and more widely spaced than the NFS pine trees. Also, the SFS is oriented towards the sun, which is expected to reduce the shading of intercanopy locations by the nearby shrub canopy. The difference in shading between the intercanopy locations on the two hillslopes helps explain why their soil moisture differs during dry periods. It also helps explain why the canopy and intercanopy cases have more similar soil moisture on the NFS than the SFS.

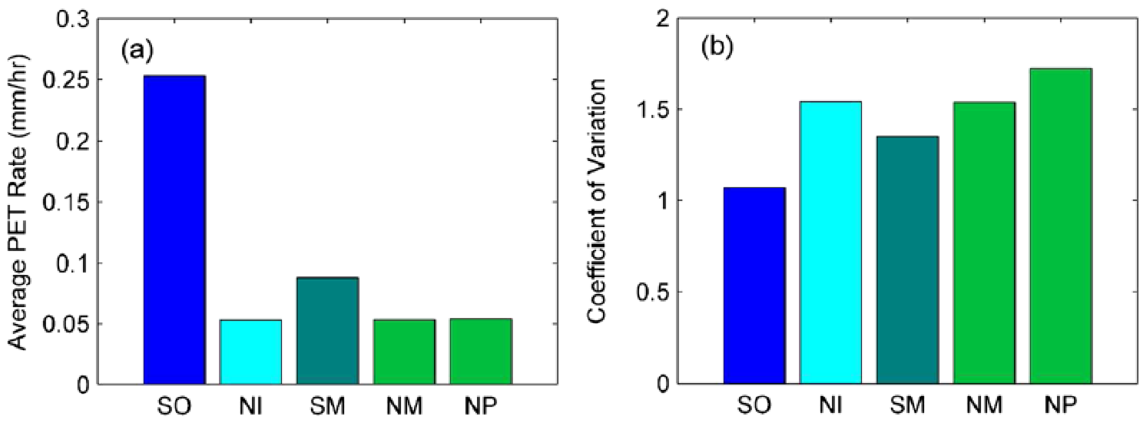

Figure 17. (a) Average and (b) coefficient of variation of hourly potential evapotranspiration (PET) rate (including both day and night) for the available location types.

Finally, it was hypothesized that soil properties also help produce the observed differences in soil moisture. The results do not support this hypothesis. Table 2 shows that the soils have more silt and less sand under both vegetation types than at intercanopy locations, but this change has only a small effect on the inferred hydraulic properties. Similarly, greater water repellency occurs for canopy locations than intercanopy locations and on the NFS than on the SFS, but the average water repellency is low for all cases. As a result, differences in soil properties are not expected to have a strong effect on the observed differences in soil moisture.

Table 2. Average percent sand, silt and clay along with saturated hydraulic conductivity (K_s) and pore disconnectedness (γ) for the south-facing intercanopy (SI), south-facing mountain mahogany (SM), north-facing intercanopy (NI) and north-facing ponderosa pine (NP) location types.

Location type	Sand (%) (+/−)	Silt (%) (+/−)	Clay (%) (+/−)	K_s (mm h^{-1})	γ
SI	68.5 (7.0)	20.7 (3.9)	10.8 (4.1)	39.6	12.2
SM	66.7 (1.4)	23.1 (1.0)	10.2 (0.9)	38.0	12.0
NI	66.4 (2.1)	25.3 (2.1)	8.3 (2.9)	38.8	11.4
NP	62.8 (3.2)	27.1 (2.3)	10.1 (1.0)	33.9	12.0

5.6 The EMT+VS Model

This study generalized the EMT model to allow it to accept fine-resolution data for vegetation and soil properties based on the hypothesis that consideration of the spatial variations in vegetation and soil characteristics would improve the model's ability to downscale soil moisture patterns (Ranney and Niemann, 2015). When vegetation cover is included in the EMT+VS model at the Cache la Poudre catchment, its performance is better than that of the EMT model. Adding vegetation increases the average NSCE from 0.080 to 0.134 at the 15 m resolution. The EMT+VS model and the EOF method both show improvements when vegetation data are provided. The EMT+VS model has greater improvements than the EOF method, suggesting that the representation of vegetation in the EMT+VS model is superior to the linear regressions used in the EOF method. Figure 18 shows the results of the various models for a date with a typical observed soil moisture pattern at the Cache la Poudre catchment. The soil moisture patterns from the EMT and EMT+VS models are substantially different. The EMT+VS pattern is more realistic because it captures the wetter conditions in the western part of the catchment and more of the local variability, particularly on the SFS. The main influences vegetation has on the soil moisture at the Cache la Poudre catchment are a reduction in soil evaporation and consequently an increase in transpiration. The addition of fine-resolution variations in vertical saturated hydraulic conductivity ($K_{s,v}$) and porosity (ϕ) play a small role in determining the soil moisture patterns at Cache la Poudre. Overall, the addition of soil data either degraded or slightly improved the model performances. In contrast, the addition of fine-resolution vegetation data improved the results of the model and proved to be a promising direction for improving soil moisture downscaling methods. These results are also expressed in terms of the NSCE and root mean square error (RMSE), shown in Table 3.

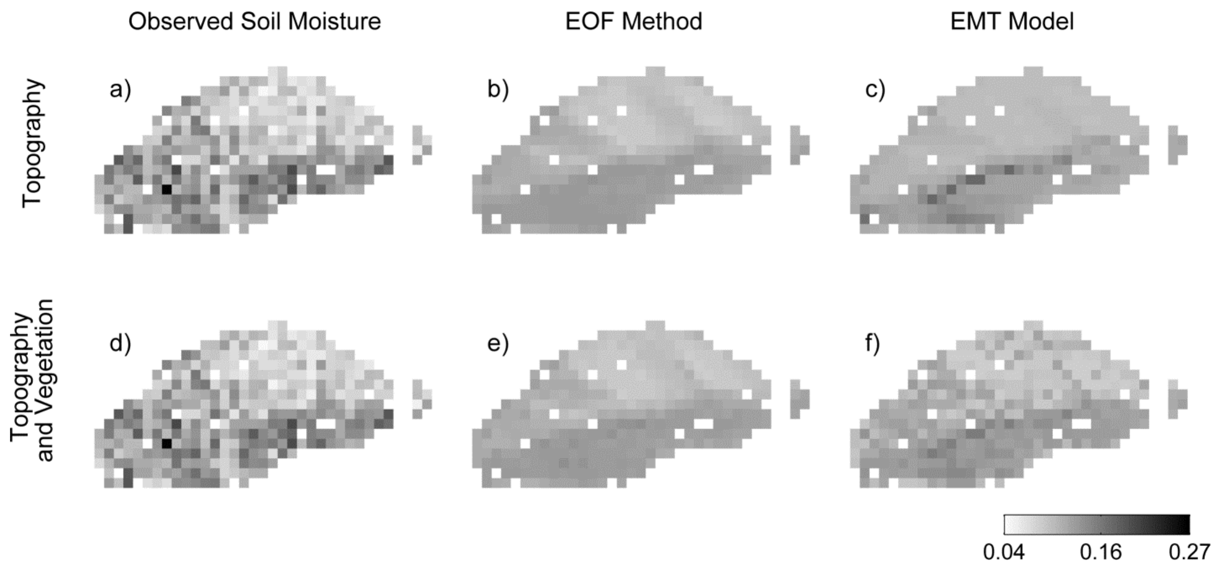

Figure 18. The first column shows the observed soil moisture pattern on an example date with intermediate moisture (June 12, 2008) at Cache la Poudre, the second column shows the soil moisture patterns that are downscaled by the EOF method, and the third column shows the soil moisture patterns that are downscaled by the (c) EMT and (f) EMT+VS models. In the top row, only fine-scale topographic information is used. In the bottom row, both fine-scale topographic and vegetation information are used. All patterns are on a 15 m grid.

Table 3. Measures of model performance when the downscaling models are supplied with various fine-resolution datasets and applied to Cache la Poudre. The NSCE, RMSE, and MRE are calculated separately for each date in the dataset and the averages, maximums, and minimums are determined from the different dates.

Grid	Scenario	Model	NSCE			RMSE	MRE
			Avg.	Max.	Min.	Avg.	Avg.
15 m	Topography	EMT	0.080	0.183	-0.027	0.031	0.453
		EOF	0.116	0.288	-0.050	0.030	0.438
	Topography and Vegetation	EMT+VS	0.134	0.375	-0.099	0.030	0.430
		EOF	0.129	0.320	-0.070	0.030	0.434
30 m	Topography	EMT	0.099	0.227	0.015	0.030	0.485
		EOF	0.172	0.399	-0.030	0.029	0.448
	Topography and Vegetation	EMT+VS	0.187	0.498	-0.089	0.029	0.463
		EOF	0.190	0.405	0.008	0.028	0.453
	Topography, Veg., and Soil	EMT+VS	0.196	0.495	-0.080	0.028	0.457
		EOF	0.226	0.391	0.050	0.027	0.437

For the Cache la Poudre catchment, the patterns of variation that are used to estimate the soil moisture in the EMT and EMT+VS models are shown in Figure 19. The deep drainage index

(DDI), which is not present in the EMT model, depends on the vegetation cover due to vegetation's role in interception. It has larger values on the SFS where the sparse vegetation reduces interception. The EMT+VS model would produce patterns that are wetter on the SFS than the NFS for wet conditions when deep drainage dominates. In the same conditions, the EMT model would produce uniform soil moisture. The radiative ET index (REI) pattern in the EMT+VS model and the ETI pattern in the EMT model are analogous, but the REI pattern in the EMT+VS incorporates vegetation, which introduces more local variability.

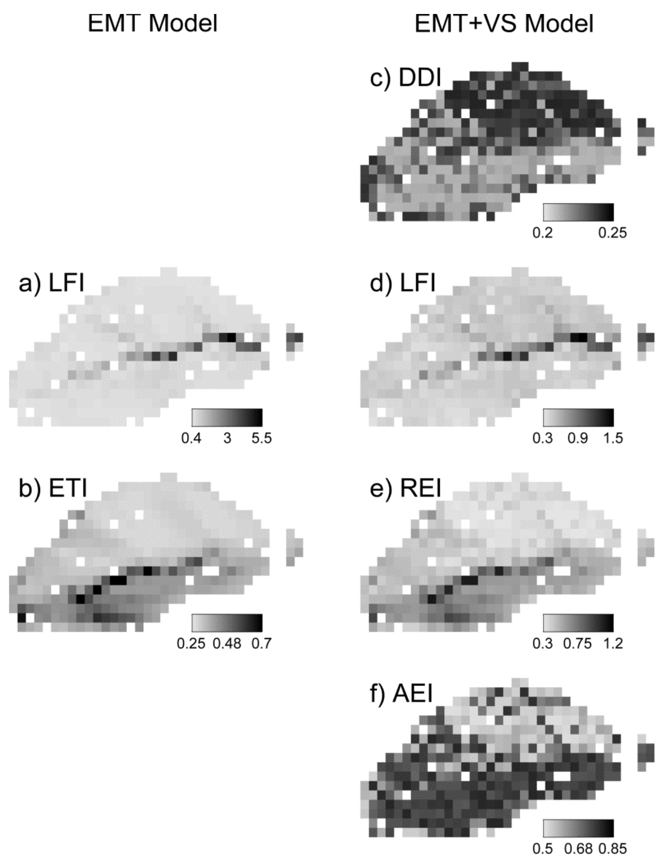

Figure 19. The first column shows the calibrated patterns of variation that are used to downscale soil moisture in the EMT model, and the second column shows the calibrated patterns of variation that are used in the EMT+VS model. Deep drainage and aerodynamic ET produce spatially constant soil moisture in the EMT model, so only two patterns are used. The index related to radiative ET in the EMT model is termed ETI while it is termed REI in the EMT+VS model. All patterns are on a 15 m grid.

The aerodynamic ET index (AEI), which is only in the EMT+VS model, depends only on vegetation cover. It has larger values on the NFS and where vegetation cover is thicker on the western portion of the Cache la Poudre catchment. From the figure, one can observe how the additional patterns of variation modeled by the EMT+VS increase the model’s ability to accurately estimate soil moisture and local variability compared to the EMT model.

As was previously mentioned, the downscaling methods were also applied to other catchments to evaluate the EMT+VS model’s use of fine resolution soil data. Figure 20 presents the application of the EOF method, EMT model, and EMT+VS model to the Nerrigundah catchment. It should be noted that fine-resolution vegetation data were not available at this catchment, so the downscaling methods were evaluated assuming a constant vegetation cover. For an example date with intermediate moisture (Figure 20a), the observed soil moisture pattern

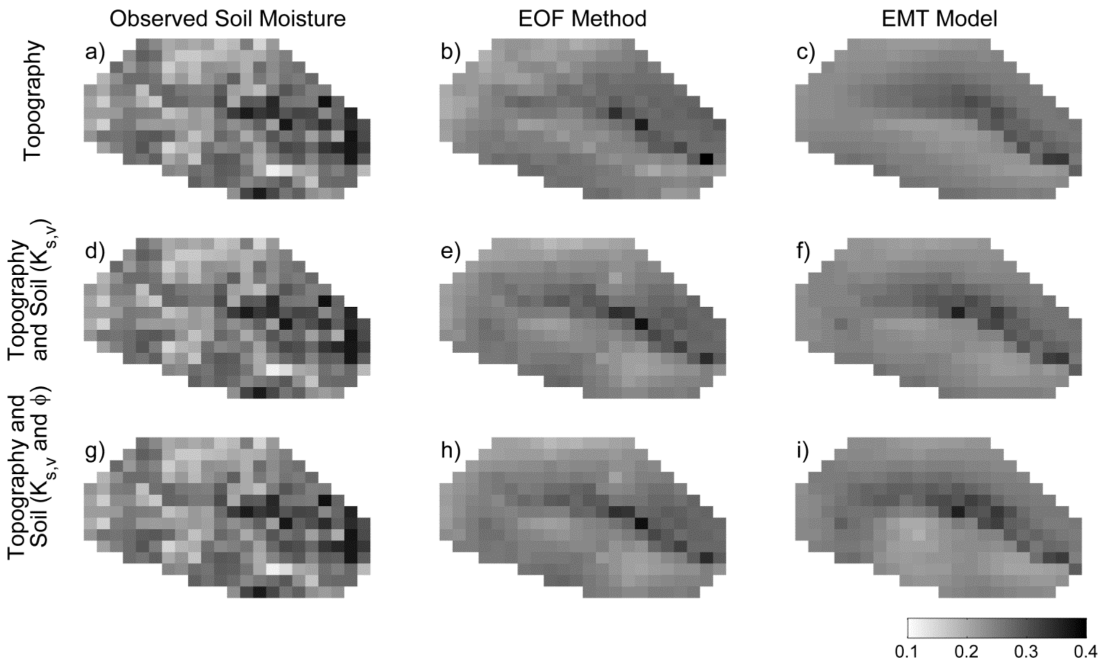

Figure 20. The first column shows the soil moisture pattern that is observed at Nerrigundah on an example date with intermediate conditions (September 12, 1997), the second column shows the soil moisture patterns that are downscaled by the EOF method, and the third column shows the soil moisture patterns that are downscaled by the (c) EMT and (f,i) EMT+VS models. In the top row, only fine-scale topographic information is used. In the middle row, fine-scale topographic and $K_{s,v}$ data are used. In the bottom row, fine-scale topographic, $K_{s,v}$, and φ data are used.

exhibits wetter conditions on the SFS than the NFS in the eastern half of the catchment. The western half of the catchment is generally drier and exhibits little dependence on hillslope orientation. When only topographic data are used in the EOF method and the EMT model, the downscaled patterns also exhibit the wetter conditions for the SFS than the NFS. However, the difference between the eastern and western halves of the catchment is not well reproduced. When the $K_{s,v}$ data are added to the EOF method and EMT+VS model, the downscaled patterns exhibit more distinct dry regions on the NFS, which corresponds to areas of higher $K_{s,v}$. The EMT+VS pattern is determined primarily by the REI and DDI. Because the DDI depends on $K_{s,v}$, the downscaled pattern reflects the $K_{s,v}$ pattern to a certain extent. The average performance from all dates (Table 4) indicates the EOF method performance improves when the

Table 4. Measures of model performance when the downscaling models are supplied with various fine-resolution datasets and applied to Nerrigundah. The NSCE, RMSE, and MRE are calculated separately for each date in the dataset and then the averages, maximums, and minimums are determined from the different dates.

Scenario	Model	NSCE			RMSE	MRE
		Avg.	Max.	Min.	Avg.	Avg.
Topography	EMT	0.182	0.222	0.143	0.048	0.165
	EOF	0.274	0.326	0.087	0.045	0.155
Topography and Soil ($K_{s,v}$)	EMT+VS	0.218	0.281	0.088	0.047	0.161
	EOF	0.291	0.348	0.178	0.045	0.151
Topography and Soil ($K_{s,v}$ and ϕ)	EMT+VS	0.115	0.282	-0.022	0.050	0.170
	EOF	0.291	0.348	0.178	0.045	0.151

similar dry regions, they do not exactly align with the dry areas in the downscaled pattern. It is possible that the EMT+VS model is capturing some soil moisture variations that are due to ϕ variations, but that the interpolated ϕ map does not correctly identify the configuration of those variations. The average performance of the EOF method is unchanged from the previous case (Table 4), but the average performance of the EMT+VS model decreases when the ϕ dataset is included. In fact, the performance of the EMT+VS model is worse for this case than the EMT model. Overall, the results suggest that the use of fine-resolution soil data for downscaling is somewhat problematic.

6. Summary of Key Results and Future Directions for Research

Overall, this study produced a new downscaling method called the EMT or EMT+VS model. This downscaling method can produce soil moisture patterns at the resolutions that are required for multiple military and civilian applications. To perform the downscaling, the method requires coarse resolution soil moisture, which is available from weather forecasting models and remote-sensing methods, and fine resolution topographic data, which is globally available. In addition, if fine resolution vegetation and soil data are available, such datasets can also be used.

This downscaling method has similar but slightly worse performance than the pre-existing EOF method when large soil moisture datasets are available for method calibration. However, for more realistic scenarios when few observations are available for calibration, the EMT model outperforms the EOF method. In addition, adequate performance can be achieved for the EMT model when relatively few calibration points are available, so the method appears to have numerous practical applications. The EMT model framework was also used to understand why certain catchments exhibit valley-dependent soil moisture patterns and others exhibit hillslope-dependent patterns. It was also use to understand why some catchments exhibit a switching between these structures through time, which produces temporally unstable soil moisture patterns. The EMT model was also shown to be able to reproduce soil moisture patterns for all of these cases.

Future research should consider three issues. First, methods should be developed to estimate model parameters when calibration data are not available. This research should aim to identify global climate, soil, and vegetation datasets that can provide information for the required model parameters. The use of such datasets should be evaluated by testing the method at the research catchments used for the previous work and potentially new catchments. Second, the model should be evaluated when multiple coarse-resolution grid cells are provided as inputs. In all studies to date, only a single coarse grid cell was provided as input. Boundaries between the coarse grid cells might introduce artifacts in the model's soil moisture output. Research should be conducted to develop a method for generating smooth variations in the estimated soil moisture pattern when provided with a grid of coarse soil moisture values. Third, methods should be developed and evaluated that can assimilate estimates from the EMT+VS model and other resources (such as from drones and/or remote-sensing methods) into a potentially superior soil moisture product.

References

Bartlett MS. 1950. Tests of Significance in factor analysis. *British Journal of Psychology Statistics Section* **3**: 77-85.

Bastiaanssen W, Pelgrum H, Wang J, Ma Y, Moreno J, Roerink G, Van der Wal T. 1998. A remote sensing surface energy balance algorithm for land (SEBAL): Part 2: Validation. *Journal of Hydrology* **212**: 213-229.

Beven KJ, Kirkby MJ. 1979. A physically based, variable contributing area model of basin hydrology. *Hydrological Sciences Bulletin* **24**: 43-69.

Bishop CM. 2006. *Pattern Recognition and Machine Learning*, 1st edition. Springer, New York.

Busch FA, Niemann JD, Coleman ML. 2012. Initial evaluation of an empirical orthogonal function-based method to downscale soil moisture patterns based on topographical attributes. *Hydrological Processes* **26**: 2696-2709.

Coleman ML, Niemann JD. 2012. An evaluation of nonlinear methods for estimating catchment-scale soil moisture patterns based on topographic attributes. *Journal of Hydroinformatics* **14**: 800-814.

Coleman ML, Niemann JD. 2013. Controls on topographic dependence and temporal instability in catchment-scale soil moisture patterns. *Water Resources Research* **49**: 1625-1642.

Dempster AP, Laird NM, Rubin DB. 1977. Maximum likelihood from incomplete data via EM algorithm. *Journal of Royal Statistical Society, Series B–Methodology* **39**: 1–38.

Dingman SL. 2002. Physical Hydrology, 2nd ed: 646 pp. Prentice Hall, Upper Saddle River, New Jersey.

Entekhabi D, Rodriguez-Iturbe I, Castelli F. 1996. Mutual interaction of soil moisture state and atmospheric processes. *Journal of Hydrology* **184**: 3-17.

Entekhabi D, Njoku EG, O'Neill PE, Kellogg KH, Crow WT, Edelstein WN, Entin JK, Goodman SD, Jackson TJ, Johnson J, Kimball J, Piepmeier JR, Koster RD, Martin N, McDonald KC, Moghaddam M, Moran S, Reichle R, Shi JC, Spencer MW, Thurman SW, Leung T, Van Zyl J. 2010. The Soil Moisture Active Passive (SMAP) Mission. *Proceedings of the IEEE* **98**: 704-716.

Erskine RH, Green TR, Ramirez JA, Macdonald LH. 2007. Digital elevation accuracy and grid cell size: Effects on estimated terrain attributes. *Soil Science Society of America Journal* **71**: 1371–1380.

Famiglietti JS, Rudnicki JW, Rodell M. 1998. Variability in surface moisture content along a hillslope transect: Rattlesnake Hill, Texas. *Journal of Hydrology* **210**: 259–281.

Fang B, Lakshmi V. 2014. Soil moisture at watershed scale: Remote sensing techniques. *Journal of Hydrology* **516**: 258-272.

Fitzjohn C, Ternan JL, Williams AG. 1998. Soil moisture variability in a semi-arid gully catchment: implications for runoff and erosion control. *CATENA* **32**: 55-70.

Green TR, Erskine RH. 2004. Measurement, scaling, and topographic analyses of spatial crop yield and soil water content. *Hydrological Processes* **18**: 1447-1465.

Green TR, Salas JD, Martinez A, Erskine RH. 2007. Relating crop yield to topographic attributes using Spatial Analysis Neural Networks and regression. *Geoderma* **139**: 23-37.

Heimsath AM, Dietrich WE, Nishiizumi K, Finkel RC. 1999. Cosmogenic nuclides, topography, and the spatial variation of soil depth. *Geomorphology* **27**: 151-172.

Johnson RA, Wichern DW. 2002. Applied Multivariate Statistical Analysis. Prentice Hall: Upper Saddle River, New Jersey.

Kerr YH, Waldteufel P, Wigneron JP, Martinuzzi J, Font J, Berger M. 2001. Soil moisture retrieval from space: the Soil Moisture and Ocean Salinity (SMOS) mission. *Geoscience and Remote Sensing, IEEE Transactions on* **39**: 1729-1735.

Korres W, Koyama CN, Fiener P, Schneider K. 2010. Analysis of surface soil moisture patterns in agricultural landscapes using Empirical Orthogonal Functions. *Hydrology and Earth System Sciences* **14**: 751–764.

Lehman BM, Niemann JD. 2008. Spatial patterns of a semi-arid montane catchment with aspect-dependent vegetation. Paper presented at *1st International Conference on Hydropedology*, State College, Pennsylvania.

Li L, Gaiser PW, Gao B-C, Bevilacqua RM, Jackson TJ, Njoku EG, Rudiger C, Calvet J-C, Bindlish R. 2010. WindSat global soil moisture retrieval and validation. *Geoscience and Remote Sensing, IEEE Transactions on* **48**: 2224-2241.

McKenzie NJ, Ryan PJ. 1999. Spatial prediction of soil properties using environmental correlation. *Geoderma* **89**: 67-94.

McLachlan G, Peel D. 2000. *Finite Mixture Models*. John Wiley & Sons, New York.

Merlin O, Escorihuela MJ, Mayoral MA, Hagolle O, Al Bitar A, Kerr Y. 2013. Self-calibrated evaporation-based disaggregation of SMOS soil moisture: An evaluation study at 3km and 100m resolution in Catalunya, Spain. *Remote Sensing of Environment* **130**: 25-38.

Minansy B, McBratney AB. 2006. A conditioned Latin hypercube method for sampling in the presence of ancillary information. *Computers and Geosciences* **32**: 1378-1388.

Moore ID, Norton TW, Williams JE. 1993. Modelling environmental heterogeneity in forested landscapes. *Journal of Hydrology* **150**: 717–747.

Nadaraya EA. 1964. On estimating regression. *Theory Probability Application* **9**: 141-142.

Nash JE, Sutcliffe JV. 1970. River flow forecasting through conceptual models part I–A discussion of principles. *Journal of Hydrology* **10**: 282–290.

Njoku EG, Jackson TJ, Lakshmi V, Chan TK, Nghiem SV. 2003. Soil moisture retrieval from AMSR-E. *Geoscience and Remote Sensing, IEEE Transactions on* **41**: 215-229.

Perry MA, Niemann JD. 2007. Analysis and estimation of soil moisture at the catchment scale using EOFs. *Journal of Hydrology* **334**: 388-404.

Perry MA, Niemann JD. 2008. Generation of soil moisture patterns at the catchment scale by EOF interpolation. *Hydrology and Earth System Sciences* **12**: 39-53.

Priestley CHB, Taylor RJ. 1972. On the assessment of surface heat flux and evaporation using large scale param. *Monthly Weather Review* **100**:81–92.

Ranney KJ, Niemann JD, Lehman BM, Green TR, Jones AS. 2015. A method to downscale soil moisture to fine-resolutions using topographic, vegetation, and soil data. *Advances in Water Resources*, in press.

Ranney KJ. 2014. A method to downscale soil moisture to fine-resolutions using topographic, vegetation, and soil data. *Thesis*. Colorado State University.

Rodriguez-Iturbe I. 2000. Ecohydrology: a hydrologic perspective of climate-soil-vegetation dynamics. *Water Resources Research* **36**: 3-9.

Roy JL, McGill WB. 2002. Assessing soil water repellency using the molarity of ethanol droplet (MED) test. *Soil Science* **167**: 83–97.

Scott C, Bastiaanssen W, Ahmad M. 2003. Mapping root zone soil moisture using remotely sensed optical imagery. *Journal of Irrigation and Drainage Engineering* **129**: 326-335.

Shin HS, Salas JD. 2000. Spatial analysis of hydrologic and environmental data based on artificial neural networks. In: *Artificial Neural Networks in Hydrology* (RS Govindaraju & AR Rao, eds). Kluwer Academic, Dordrecht. 259-286.

Tarboton DG, Schreuders KT, Watson DW, Baker ME. 2009. Generalized terrain based flow analysis of digital elevation models. In *18th World IMACS Congress and MODSIM09 International Congress on Modelling and Simulation*, Anderson RS, Braddock RD, Newham LTH, Modelling and Simulation Society of Australia and New Zealand and International Association for Mathematics and Computers in Simulation: Cairns, Australia. July 2009:2000-2006.

Temimi M, Leconte R, Chaouch N, Sukumal P, Khanbilvardi R, Brissette F. 2010. A combination of remote sensing data and topographic attributes for the spatial and temporal monitoring of soil wetness. *Journal of Hydrology* **388**: 28–40.

Traff DC, Niemann JD, Middlekauff SA and Lehman BM. 2014. Effects of woody vegetation on shallow soil moisture at a semiarid montane catchment. *Ecohydrology*.

Walker JP. 1999. Estimating soil moisture profile dynamics from near-surface soil moisture measurements and standard meteorological data. *Dissertation*. University of Newcastle.

Walker JP, Willgoose GR, Kalma JD. 2001. The Nerrigundah dataset: Soil moisture patterns, soil characteristics, and hydrological flux measurements. *Water Resources Research* **37**: 2653-2658.

Watson GS. 1964. Smooth regression analysis. *Sankhya Indian Journal of Statistics* **26**: 359-372.

Werbylo KL, Niemann JD. 2014. Evaluation of Sampling Techniques to characterize topographically-dependent variability for soil moisture downscaling. *Journal of Hydrology* **516**: 304-316.

Western AW, Grayson RB. 1998. The Tarrawarra dataset: soil moisture patterns, soil characteristics, and hydrological flux measurements. *Water Resources Research* **34**: 2765-2768.

Western AW, Grayson RB, Blöschl G, Willgoose GR, McMahon, TA. 1999. Observed spatial organization of soil moisture and its relation to terrain indices. *Water Resources Research* **35**: 797–810.

Western AW. 2001. Toward capturing hydrologically significant connectivity in spatial patterns. *Water Resources Research* **37**: 83.

Wilson DJ, Western AW, Grayson RB, Berg AA, Lear MS, Rodell M, Famiglietti JS, Woods RA, McMahon TA. 2003. Spatial distribution of soil moisture over 6 and 30 cm depth, Mahurangi river catchment, New Zealand. *Journal of Hydrology* **276**: 254-274.

Wilson DJ, Western AW, Grayson RB. 2005. A terrain and data-based method for generating the spatial distribution of soil moisture. *Advances in Water Resource*s **28**: 43-54.

Worsham L, Markewitz D, Nibbelink NP, West LT. 2012. A comparison of three field sampling methods to estimate soil carbon content. *Forest Science* **58**: 513–522.

Zreda M, Desilets D, Ferré TPA, Scott RL. 2008. Measuring soil moisture content non-invasively at intermediate spatial scale using cosmic-ray neutrons. *Geophysical Research Letters* **35**: L21402.